공학석사 학위논문

The Effects of Rare Earth Elements on High Pressure Die Casting Mg Alloys

2019 년 2 월

서울대학교 대학원

공과대학 재료공학부

LUAN FEIFEI

The Effects of Rare Earth Elements on High Pressure Die Casting Mg Alloys

지도교수 신광선

이 논문을 공학석사학위논문으로 제출함

2019 년 1월

서울대학교 대학원

공과대학 재료공학부

LUAN FEIFEI

LUAN FEIFEI의 석사학위논문을 인준함

2019 년 1 월

위 원 장 정 인 호 (인)

부 위 원 장 신 광 선 (인)

위 원 이 명 규 (인)

Abstract

The Effect of Rare Earth Elements on High-Pressure Die-casting Mg alloys

Feifei Luan

School of Materials Science and Engineering

The Graduate School

Seoul National University

Magnesium is the 12th element in the element pool, the 8th abundant element in the earth. It attracted many researchers applied on structural materials because of its low density. As the lightest structural materials, magnesium alloys are very suitable for the applications of automotive industry where vehicle weight reduction and consequently energy saving are becoming the word focus. It is well known that the possible application of AZ91 and AM60 alloys is still restricted due to some problems. For example, the two alloys are unsuitable for manufacturing parts operating at temperatures higher than 120 °C. In addition, the strength and ductility of the commercial AZ91 and AM60 alloys do not simultaneously satisfy the requirement of some important parts. For example, AZ91 alloy's strength is relatively high; however, the ductility of the alloy is not so good due to the high Al content. Although AM60 alloy has a high ductility, its strength is relatively poor. Various alloying and/or micro-alloying elements, such as Ce, Nd, Y, Si, Ca, Ti, B, Sr, Sb, Bi, Pr and so on, have been chosen to further improve the mechanical

properties of AZ91 alloy. With the addition of yttrium, the AZ91D alloy is found to have good mechanical properties with the tensile strength of 270 MPa and elongation of 11%. For the modified-AM60 alloys, various alloying and/or micro-alloying elements, such as Ca, Sn, Y, Si, Ti, Ag, Nd, B, RE, Sr, Ce and so on, have been chosen to further enhance the mechanical properties of AM60 alloys.

In this article, the effect of rare earth elements on commercial Mg alloys were observed. For developing high strength die casting Mg alloys, various RE elements were used for precipitating new phase to achieve the goal. Tensile test, corrosion test and other mechanical test was carried out, and SEM and EDS was used for the analysis of section part.

In the first part, the process of developing new alloys will be introduced and the influence of different elements on Mg alloys will be compared as well. Sr, Y, Sn, Ca and Zn were added into Mg-Al based alloys. The specimen was produce 350t cold chamber die-casting machine.

In the second part, the practical die casting process and parameters will be introduced. The strength and elongation was observed. Microstructure was observed by SEM and OM. Then phase and precipitate were observed by EDS and XRD. Compared with simulated results, the phase was observed as expcted.

At last, the specimen were heat treated at 120 ^{o}C for 0.5h to 12h. After heat treatment, the mechanical properties was improved, and due to different phase in different alloys, some properties was improved significantly.

Keywords: High Pressure Die Casting, Mg-Al Based Alloy, Mechanical Property

Contents

List of Tables

List of Figures

The Effect of Rare Earth Elements on High-Pressure Die-casting Mg alloys

I. Introduction

1.1 Mg Alloys

Magnesium is the 12th element in the element pool, the 8th abundant element in the earth. It attracted many researchers applied on structural materials because of its low density. As the lightest structural materials, magnesium alloys are very suitable for the applications of automotive industry where vehicle weight reduction and consequently energy saving are becoming the word focus [1,2]. It is well known that the applications of magnesium alloys are significantly potential in automobile, aircraft, aerospace, and 3C industries because of their low density, high specific strength, good castability and better damping capacity and so on [3].

It is well known that the possible application of AZ91 and AM60 alloys is still restricted due to some problems. For example, the two alloys are unsuitable for manufacturing parts operating at temperatures higher than 120 °C. In addition, the strength and ductility of the commercial AZ91 and AM60 alloys do not simultaneously satisfy the requirement of some important parts [3]. For example, AZ91 alloy's strength is relatively high; however, the ductility of the alloy is not so good due to the high Al content. Although AM60 alloy has a high ductility, its strength is relatively poor. As shown in Table 1.1, various alloying and/or micro-alloying elements, such as Ce, Nd, Y, Si, Ca, Ti, B, Sr, Sb, Bi, Pr and so on, have

been chosen to further improve the mechanical properties of AZ91 alloy. With the addition of yttrium, the AZ91D alloy is found to have good mechanical properties with the tensile strength of 270 MPa and elongation of 11%. For the modified-AM60 alloys, various alloying and/or micro-alloying elements, such as Ca, Sn, Y, Si, Ti, Ag, Nd, B, RE, Sr, Ce and so on, have been chosen to further enhance the mechanical properties of AM60 alloys [4,5]. Although a lot of modified-AZ91 and AM60 casting magnesium alloys with various additions have been developed in recent years, these works mainly focus on the tensile properties, strengthening mechanism and/or corrosion resistance. The investigation on the fatigue properties of the modified-AZ91 and AM60 alloys with various additions is still limited.

Table 1.1 As-cast RT tensile properties of modified-AM60 alloys with various additions

Compositions (wt%)	Casting processes	UTS (MPa)	YS (MPa)	δ (%)
AM60 + 0.2Ti	PM	284	–	11.2
AM60 + 0.4Ti	PM	276	–	9.8
AM60 + 0.5Sn	Squeeze casting	182	–	10.0
AM60 + 4.0Sn	Squeeze casting	212	–	8.1
AM60 + 1Sn+0.3Ti	Squeeze casting	190	115	9.3
AM60 + 1Sn+0.3Ti+0.5Ag	Squeeze casting	250	123	9.0
AM60 + 1Sn+0.3Ti+1.0Ag	Squeeze casting	265	128	8.8
AM60 + 1.8Si+0.32Ca	PM	182	–	8.5
AM60 + 0.9Y	PM	192	62	12.6
AM60 + 0.9Nd	PM	230	127	14.0
AM60 + 0.15B	PM	160	–	5.7
AM60 + 1.6RE	PM	170	–	6.2
AM60 + 0.15B+1.6RE	PM	185	–	6.0

Table 1.2 As-cast RT mechanical properties of modified-AZ91 alloys with various additions

Compositions (wt%)	Casting processes	Tensile properties		
		UTS (MPa)	YS (MPa)	δ (%)
AZ91 + 1.0Ce	HPDC	248	158	6.8
AZ91 + 2.0Ce	HPDC	227	144	6.1
AZ91 + 1.0Nd	HPDC	258	164	5.6
AZ91 + 1.5Nd	HPDC	241	154	5.0
AZ91 + 0.5Y	HPDC	270	162	10.0
AZ91 + 0.8Y	HPDC	272	161	11.0
AZ91 + 0.032B	PM	226	110	4.8
AZ91 + 0.04B	PM	229	113	4.9
AZ91 + 1.0Bi	PM	250	166	4.6
AZ91 + 0.4Sb	PM	264	177	4.5
AZ91 + 1.0Bi+0.4Sb	PM	269	178	3.3
AZ91 + 0.8Pr	HPDC	228	137	6.8
AZ91 + 1.2Pr	HPDC	222	128	6.2
AZ91 + 1.0Ca+0.5Sr	HPDC	250	–	3.5
AZ91 + 0.5Ti	PM	170	140	4.0
AZ91 + 1.0Y+1.0Ca	HPDC	232	168	3.7
AZ91 + 1.0Y+1.5Ca	HPDC	241	183	3.2
AZ91 + 0.2Si+0.2Sb	HPDC	231	135	5.8
AZ91 + 0.5Si+0.2Sb	HPDC	224	126	3.7

In recent years, although a lot of positive results about the modified-AZ91, AM60 and WE43 casting magnesium alloys with various additions, Mg–Al/Zn/Sn based low cost casting magnesium alloys, Mg–Gd/Nd based high strength casting magnesium alloys and purification technologies for reducing impurity elements in casting magnesium alloys, have been obtained, the following studies still need to be further carried out [6]. Further investigations need to be considered in order to better understand the effect of various alloying and micro-alloying elements on the microstructure, mechanical properties, corrosion resistance and/or castability of casting magnesium alloys, and then determine the optimal chemical compositions. The effects of heat treatment on the microstructure, mechanical properties and corrosion resistance of the new alloys are also needed to be further investigated [7].

For a broader application in automobile parts for casting magnesium alloys, a good knowledge of fatigue properties, such as fatigue curves for constant and

variable amplitude loading, their scatters, influence of mean stresses and notches on fatigue strength as well as the influence of thickness and surface (casting skin), is very necessary. The casting process of casting magnesium alloys for the actual automobile parts, such as selection of casting methods (including PM, HPDC, LPDC, LPSC, LPSMC, squeeze casting, sand casting and so on), mold design, optimization of technological parameters (pouring temperature, pouring rate and so on), sectional sensitivity and casting defects, needs to be systematically investigated. For wider application of casting magnesium alloys, more systematical investigation on mechanical properties at elevated temperatures and development of heat-resistant magnesium alloys is very crucial.

1.2 Die Casting

Die casting is a metal casting process that is characterized by forcing molten metal under high pressure into a mold cavity. The mold cavity is created using two hardened tool steel dies which have been machined into shape and work similarly to an injection mold during the process. Most die castings are made from non-ferrous metals, specifically zinc, copper, aluminum, magnesium, lead, pewter, and tin-based alloys. Depending on the type of metal being cast, a hot- or cold-chamber machine is used [9,10].

The casting equipment and the metal dies represent large capital costs and this tends to limit the process to high-volume production. Manufacture of parts using die casting is relatively simple, involving only four main steps, which keeps the incremental cost per item low. It is especially suited for a large quantity of small- to

medium-sized castings, which is why die casting produces more castings than any other casting process. Die castings are characterized by a very good surface finish (by casting standards) and dimensional consistency [10].

Two variants are pore-free die casting, which is used to eliminate gas porosity defects; and direct injection die casting, which is used with zinc castings to reduce scrap and increase yield.

Magnesium alloys are very attractive for industrial applications because of their light weighting, energy saving, and environment friendliness. As one of the most popular casting methods for processing magnesium alloys, the high pressure die casting (HPDC) process has various advantages including faster prototyping, better casting dimensional accuracy, and fewer requirements for post-processing. Compared with wrought magnesium alloys, casting magnesium alloys have clear economic advantages for mass production of components due to their shorter processing cycle and assembly costs. Therefore, casting magnesium alloys obtain more incremental use. To date, almost 90% of total application products for magnesium alloys involve casting processes. However, the applications of casting magnesium alloys are still limited. One of the main reasons is that the mechanical properties at room and elevated temperatures for the commercial casting magnesium alloys are still unsatisfactory as compared with Al alloys. Consequently, the development of casting magnesium alloys with high performance have received much global attention in recent years and many positive results, especially on the modification of the commercial casting magnesium alloys

and the development of low cost, high strength and/or creep-resistant casting magnesium alloys, have been obtained.

There are two basic types of die casting machines: hot-chamber machines and cold-chamber machines. These are rated by how much clamping force they can apply [12].

Hot-chamber die casting, also known as gooseneck machines, relies upon a pool of molten metal to feed the die. At the beginning of the cycle the piston of the machine is retracted, which allows the molten metal to fill the "gooseneck". The pneumatic- or hydraulic-powered piston then forces this metal out of the gooseneck into the die. The advantages of this system include fast cycle times (approximately 15 cycles a minute) and the convenience of melting the metal in the casting machine. The disadvantages of this system are that it is limited to use with low-melting point metals and that aluminum cannot be used because it picks up some of the iron while in the molten pool. Therefore, hot-chamber machines are primarily used with zinc-, tin-, and lead-based alloys [13, 14].

Cold-chamber die casting are used when the casting alloy cannot be used in hot-chamber machines; these include aluminum, zinc alloys with a large composition of aluminum, magnesium and copper. The processes for these machines start with melting the metal in a separate furnace. Then a precise amount of molten metal is transported to the cold-chamber machine where it is fed into an unheated shot chamber (or injection cylinder). This shot is then driven into the die by a hydraulic or mechanical piston. The biggest disadvantage of this system is the slower cycle

time due to the need to transfer the molten metal from the furnace to the cold-chamber machine [13, 14].

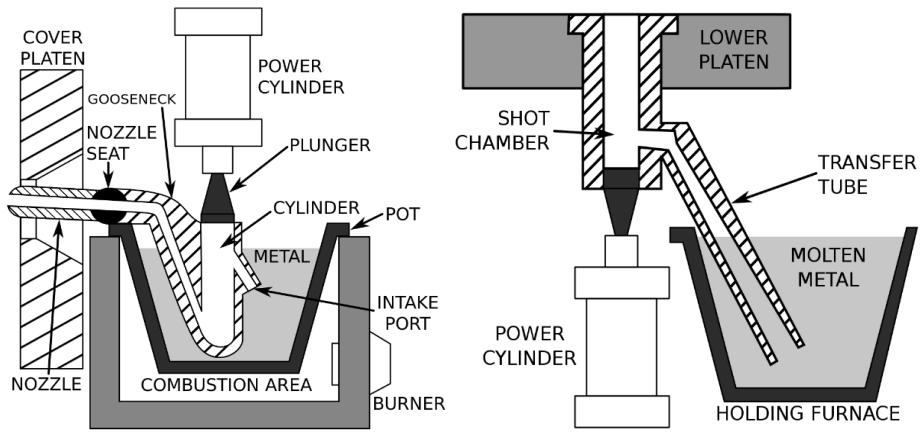

(a) (b)

Figure 1.1 Schematics of high pressure die-casting machine: (a) hot chamber type and (b) cold chamber type

The following are the four steps in traditional die casting, also known as high-pressure die casting; these are also the basis for any of the die casting variations: die preparation, filling, ejection, and shakeout. The dies are prepared by spraying the mold cavity with lubricant. The lubricant both helps control the temperature of the die and it also assists in the removal of the casting. The dies are then closed and molten metal is injected into the dies under high pressure; between 10 and 175 MPa [16]. Once the mold cavity is filled, the pressure is maintained until the casting solidifies. The dies are then opened and the shot (shots are different from castings because there can be multiple cavities in a die, yielding multiple castings per shot) is ejected by the ejector pins. Finally, the shakeout involves separating the scrap, which includes the gate, runners, sprues and flash, from the shot. This is

often done using a special trim die in a power press or hydraulic press. Other methods of shaking out include sawing and grinding. A less labor-intensive method is to tumble shots if gates are thin and easily broken; separation of gates from finished parts must follow. This scrap is recycled by remelting it. The yield is approximately 67%.

The high-pressure injection leads to a quick fill of the die, which is required so the entire cavity fills before any part of the casting solidifies. In this way, discontinuities are avoided, even if the shape requires difficult-to-fill thin sections. This creates the problem of air entrapment, because when the mold is filled quickly there is little time for the air to escape. This problem is minimized by including vents along the parting lines, however, even in a highly refined process there will still be some porosity in the center of the casting. Most die casters perform other secondary operations to produce features not readily castable, such as tapping a hole, polishing, plating, buffing, or painting.

1.3 Fracture in Die Casting

As one of the most popular casting methods for processing magnesium alloys, the high pressure die casting (HPDC) process has various advantages including faster prototyping, better casting dimensional accuracy, and fewer requirements for post-processing [17]. Because porosity is one of the main defects in die castings, studies have been conducted to reveal the correlation between porosity and mechanical properties. Some group had investigated the relationship between internal porosity and fracture strength of die-cast AM60B magnesium alloy by using the X-ray

tomography, and concluded that the local area fraction of porosity was the primary factor in determining the tensile properties of specimens [18].

The variability in tensile ductility of HPDC AM50 and AE44 magnesium alloy was studied, and the results showed that the ductility was correlated to the area fraction of porosity measured in the fracture surface, not the average volume fraction of porosity in the 3D microstructure. By employing the size and location of the porosity in fracture surfaces of die-cast AZ91 and AE44 specimens, the tensile elongation was determined with an average error of 5.3%. The effect of porosity in HPDC magnesium alloy on the ductility was studied [19]. Via a two-dimensional microstructure-based finite element modeling method, and results showed that for the regions with lower pore size and lower volume fraction, the ductility generally decreased as the pore size and pore volume fraction increase, whereas, for the regions with larger pore size and larger pore volume fraction, other factors such as the mean distance between the pores had substantial influence on the ductility [20].

Though porosity was proved to be the key factor in determining the mechanical properties in many studies, there were still studies showed that the mechanical properties were influenced by the whole microstructure not only the porosity. Some group also studied the effect of position and section thickness on the tensile properties in HPDC magnesium alloy, and suggested that the tensile properties were influenced by the average size, area fraction and clustering tendency of pores and β phase particles as well as average grain size [19, 21]. Mechanism for fatigue crack growth in HPDC magnesium alloys was studied, and results showed that

these fatigue micromechanics were manifested by the concomitant effects of casting pores, interdendritic Al-rich solid solution layer, β-phase particles, Mn-rich inclusions.

1.4 Research Objectives

1) The proper amount addition of Al to the die-cast Mg alloy with considering room temperature strength and castability.

2) Removal of thermally unstable $Mg_{17}Al_{12}$ phase by the addition of alloying elements.

3) Matrix strengthening by the addition of soluble alloying elements.

4) The addition of third and fourth alloying elements to the Mg-Al alloys in order to form thermally stable precipitates.

II. Experiment Procedure

2.1 Alloy Design

a. Mg-Al-Zn (Mg-Al-Mn) Alloys

A high pressure die-casting process shows excellent productivity due to the short cycle time. Moreover, the high pressure die-cast products exhibit enhanced mechanical properties with the refined microstructure due to the fast cooling rate. In case of die-cast Mg alloys, it is necessary to add Al to the Mg alloys due to castability. Majority of the die-cast Mg alloys are made from Mg-Al base (AM50,

AM60) and Mg-Al-Zn base (AZ91) alloys. AM50 and AM60 alloys exhibit a good combination of strength and ductility, and AZ91 alloy shows excellent castability and strength. Al is added to Mg as the prime alloying element in a high pressure die-casting process to increase the strength and castability. However, high Al contents can decrease ductility due to brittle $Mg_{17}Al_{12}$ precipitates. This precipitate can induce the formation of crack through the debonding process between the a-Mg and the $Mg_{17}Al_{12}$ phase [22]. Moreover, this phase can be easily dissolved at elevated temperature, high temperature mechanical properties are significantly decreased. Therefore, the amount of Al addition should be controlled around 6wt%~8wt% in high pressure die-cast Mg-Al alloys for high temperature applications [23].

b. Mg-Al-Ca Alloys

Ca addition, as a cheaper and lighter alternative to rare-earth elements, also contributes to high temperature properties. Calcium has the atomic weight, which is half of atomic weight of Sr and third of that of RE elements. Consequently, alloying with Ca provides maximum increase of both room temperature tensile and compressive yield strength, and especially creep strength for the equal weight percentage additions compared to Sr and RE metals [25]. Since Ca is a relatively inexpensive element, it also provides the maximum increase of the above properties in terms of value to cost. The Al_2Ca phase has stability at high temperatures and the formation of the $Mg_{17}Al_{12}$ phase is suppressed. Despite its beneficial contribution to creep properties, Ca makes the alloy prone to hot tearing

and die sticking especially when the level is above 1wt. % [24].

c. Mg-Al-RE Alloys

Rare-earth elements, in this alloy system, form at least one (in general a mixture) precipitate, which improves the creep strength due to complete suppression of the formation of $Mg_{17}Al_{12}$ precipitate. Rare-earth elements are relatively expensive and therefore a cheaper substitute known as misch metal, a mixture of several rare-earth elements that is enriched in one of the constituents is generally used. The microstructure of Mg-Al-RE alloys dictates the creep resistance of AE42 and AE44 alloys [28]. Al_4RE (also reported as $AE_{11}RE_3$) lamellar phase dominates the interdendritic microstructure, which also contains minor amounts of particulate Al_2RE phase. The RE used in AE alloys consists primarily of cerium and lanthanum, which makes the Al_4RE in the alloys a mixture of Al_4Ce and Al_4La. Since these phases are present at the grain boundaries they provide a very effective hindrance to grain boundary sliding, the dominant mechanism for creep in Mg-Al based die-cast alloys [28, 29].

Unfortunately, the thermal stability of Al_4RE phase does not extend beyond 150^{o}C. Microstructural analysis shows that the volume fraction of the Al_4RE phase decreases while that of the less stable phases Al_2RE and $Mg_{17}Al_{12}$ increases through phase transformations at higher temperatures such as 175^{o}C.

d. Mg-Al-Ca-Sr-RE Alloys

Many Al containing Mg alloy systems have been developed with combined

additions of rare-earth and alkaline earth elements. Nissan patent on an Mg-Al-Ca-RE alloy and later a Honda alloy ACM522 (Mg5%Al-2%Ca-2%RE) both claim improved creep resistance over AE42 alloy. ACM522 alloy is based on specific Al/RE/Ca ratios to insure Al-RE precipitates in additions to Al-Ca intermetallics. The microstructure of these alloys exhibit a combination of Al-RE and Al-Ca intermetallics mixtures [30]. Another example is MRI153M. MRI153M is a beryllium free, low cost creep resistant alloy with the capability of long-term operation at temperatures up to 150ºC under high stresses. MRI153M alloy exhibits the die castability similar to that of AZ91D alloy [26]. The creep properties of MRI153M, at 100~150ºC under stresses of 50~110 MPa are also significantly superior to those of commercial alloys. This makes MRI153M as a superior candidate for automotive applications such as transmission housings, oil pans, valve covers etc.

e. Mg-Al-Sn Alloys

In most recent years, Sn added Mg-Al based alloy system has been developed. The addition of Sn to die-cast Mg alloys has several advantages such as low diffusivity in Mg (10×10^{-14} m/s^2 at 400 ^oC), low solid solubility in Mg at room temperature and high solubility in Mg at 800 ^oC. Moreover, the thermally stable Mg_2Sn phase can be precipitated within matrix and along grain boundaries which has melting point of 770ºC, this phase leads to the improvement of high temperature mechanical properties in die-cast Mg-Al alloys [10, 29].

2.2 Experiment Condition

2.2.1 Die Casting Condition

The alloy was produced on a 350 ton cold chamber die-casting machine, figure 2.1(a). High pressure die-cast mold is shown in Figure 2.1(b). The alloy was molten at 680ºC under the SF_6 gas. The mold was maintained at a temperature of 280ºC, which was equipped with an oil heating/cooling system.

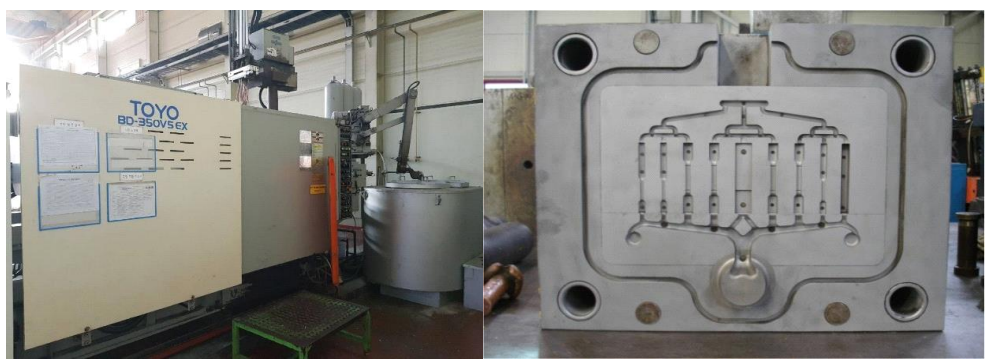

Figure 2.1 (a) 350 Ton Die Casting Machine (b) Die-cast mold

The alloying elements to the Mg-Al base alloy were Sn, Ca, Sr and Mm (Ce-rich), Mn, Zn, Y. Mg, Al and Sn, Ca, Mn, Zn and Y were melted in the form of ingot with 99.9% purity. Sr were added in the form of Al-90 wt. % Sr. The compositions of different alloy systems were shown in Table 2.1. And other parameters of HPDC were shown in Table 2.2.

Table 2.1 Alloy Compositions

Alloys	Composition (wt.%)								
	Al	Mn	Ca	Sr	Y	Sn	Zn	Mm(Ce-rich)	Mg
Mg-6.0Al-5.0Sn-0.6Ca-0.3Mn	6.0	0.6	0.6	-	-	5.0	-	-	Bal.
Mg-6.0Al-6.0Sn-0.75Ca-0.3Mn	6.0	0.6	0.75	-	-	6.0	-	-	Bal.
Mg-7.0Al-0.5Zn-0.3Y	7.0	0.3	1.0	-	0.3	-	0.5	-	Bal.
Mg-7.0Al-1.0Zn-0.3Y	7.0	0.3	1.0	-	0.3	-	1.0	-	Bal.
Mg-7.0Al-1.0Zn-0.3Y-0.5Mm	7.0	0.3	-	-	0.3	-	1.0	0.5	Bal.
Mg-8.0Al-1.0Zn-0.3Y	8.0	0.3	-	-	0.3	-	1.0	-	Bal.
Mg-8.0Al-1.0Zn-0.5Y	8.0	0.3	-	-	0.5	-	1.0	-	Bal.
Mg-8.5Al-1.0Zn-0.5Y	8.5	0.3	-	-	0.5	-	1.0	-	Bal.
Mg-7.0Al-1.0Ca-0.3Y	7.0	0.3	1.0	-	0.3	-	-	-	Bal.
Mg-8.0Al-1.0Ca-0.5Y	8.0	0.3	1.0	-	0.3	-	-	-	Bal.
Mg-8.0Al-1.0Ca-0.1Sr-0.5Y	8.0	0.3	1.0	0.1	0.5	-	-	-	Bal.
Mg-8.0Al-1.0Ca-0.3Sr-0.5Y	8.0	0.3	1.0	0.3	0.5	-	-	-	Bal.
Mg-8.0Al-2.0Zn-1.5Mm	8.0	0.3	-	-	-	-	2.0	1.5	Bal.
Mg-8.0Al-3.0Zn-1.5Mm	8.0	0.3	-	-	-	-	3.0	1.5	Bal.

Table 2.2 Die Casting Condition

Contents	Remark
Melt Temp.	680°C
Mold Temp.	200°C
Plunger Diameter (D_S)	50 mm
Slow Phase Velocity	0.2~0.35 m/s
Fast Phase Velocity	2.5 m/s
Sleeve Length (L_S)	352 mm
Vacuum Lapse Time	Variable
Slow Phase Length (L_L)	260 mm
Fast Phase Length (L_H)	78 mm
Biscuit Thickness	14 mm

2.2.2 Tensile Test Condition

The tensile tests were performed at room temperature (25°C) at an initial strain rate of 2 x 10^{-4}/s. The specimens were cylindrical shape, with gauge lengths and diameter of 16 mm and Ø 4mm. The drawing of specimen was shown in Figure 2.2 [8].

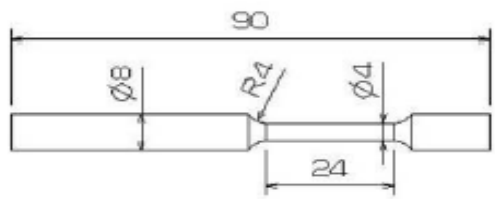

Figure 2.2 Tensile Test Specimen Dimension

2.2.3 Heat Treatment Condition

Those compositions with high elongation were selected for heat treatment. The heat treatment was carried out in 120ºC, for 0.5, 1, 2, 4, 8, 12 hours.

2.3. Characterization of microstructure and mechanical properties

2.3.1. Observation of microstructure

The specimen for observing microstructure was mechanically grinded with SiC paper from #600 to #4,000, and then polished with 0.3 and 0.05 mm alumina powder. These specimens were then etched with nital (0.5% nitric acid + distilled water). The microstructure was observed with an optical micrograph, SEM (MERLIN Compact). Quantitative analysis of various precipitates was performed with JMatPro software and EDS.

III. Results and Discussions

3.1. Thermodynamic prediction of precipitates

Thermodynamic calculation with JMatPro software was used to predict the solidification sequence and the amount of precipitates at room temperature. The solidification behaviors for investigated alloys are given in Figure 3.1. In the AM60-5.0Sn-0.6Ca alloy (Figure 3.1 (a)), the Al_8Mn_5 phase was initially precipitated, and the Mg_2Sn eutectic phase was precipitated in the last stage. The $Mg_{17}Al_{12}$ eutectic phase was not precipitated The solidification sequence of this alloy is Al_8Mn_5, α-Mg, $Al_{11}Mn_4$ Ca_2Sn, Mg_2Sn phases presented in Figure 3.1 (a). The $Mg_{17}Al_{12}$ eutectic phase was not precipitated in this alloys system (Fingure3.1 (a) and (b)). When more Ca was added, the fraction Mg_2Sn phase increased.

In the case of Mg-7.0Al-1.0Zn-0.5Mm alloy system, the Al_8Mn_5 phase was initially precipitated, and the $Mg_{17}Al_{12}$ eutectic phase was precipitated in the last stage, after adding Mm (Ce-rich), the fraction of $Mg_{17}Al_{12}$ was decreased. With the increase of Zn, Al_2Y phase increased as well. The results were shown in Figure 3.1(c) ~ (e).

In the Mg-8.0Al-1.0Zn-0.3Y alloy system, when Al was added until 8.5wt%, $Mg_{17}Al_{12}$ phase increased a lot. And use Ca instead of Zn, $Mg_{17}Al_{12}$ phase was disappeared. Al_4Sr precipitated after added Sr. and until the contents of Al was increased to 8wt%, Al_3Y was precipitated

For the last comparison, add the contents of Zn until 3wt%, the fraction of

eutectic $Mg_{17}Al_{12}$ was suppressed and $Al_{11}Mn_4$ phase increase significantly. The exact data was shown in Table 3.1.

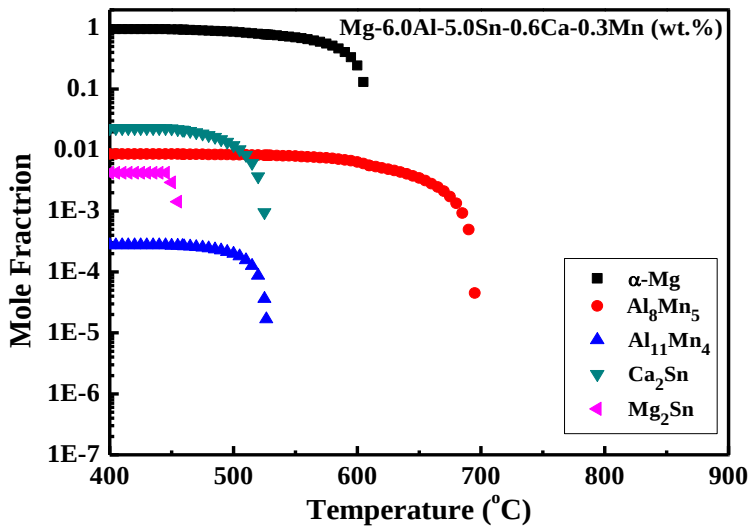

(a)

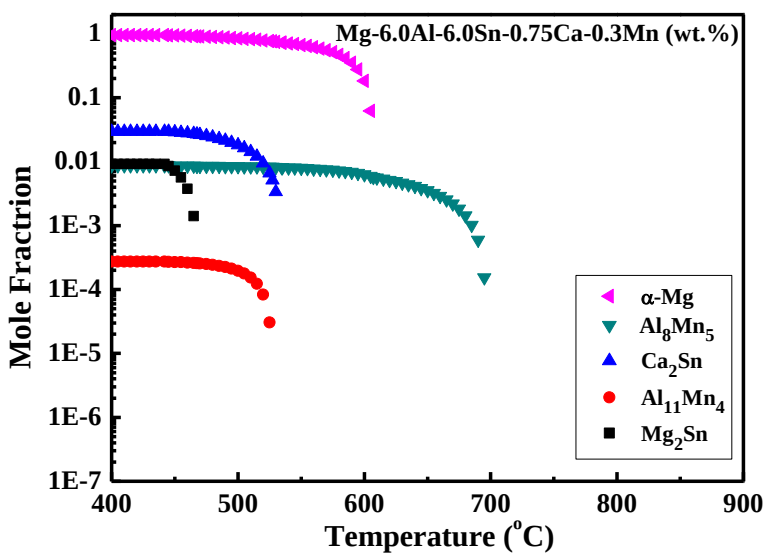

(b)

Figure 3.1 Solidification behaviors of high pressure die-cast alloys: (a) Mg-6.0Al-5.0Sn-0.6Ca-0.3Mn, (b) Mg-6.0Al-6.0Sn-0.75Ca-0.3Mn

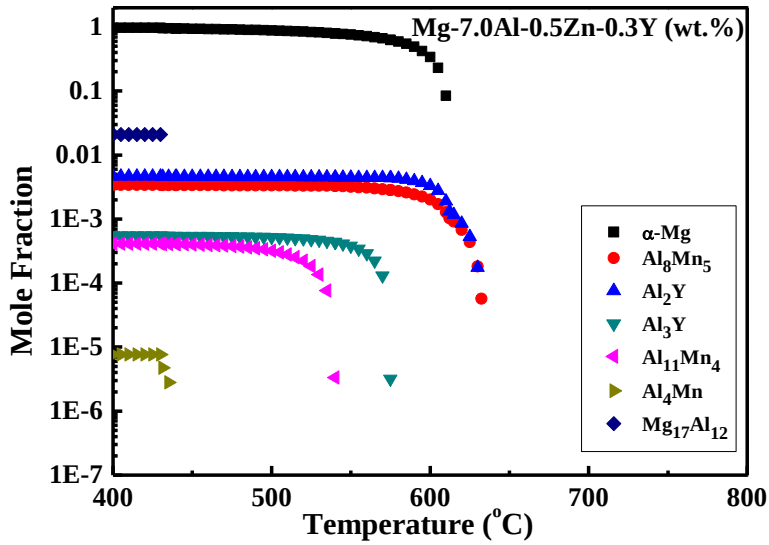

(c)

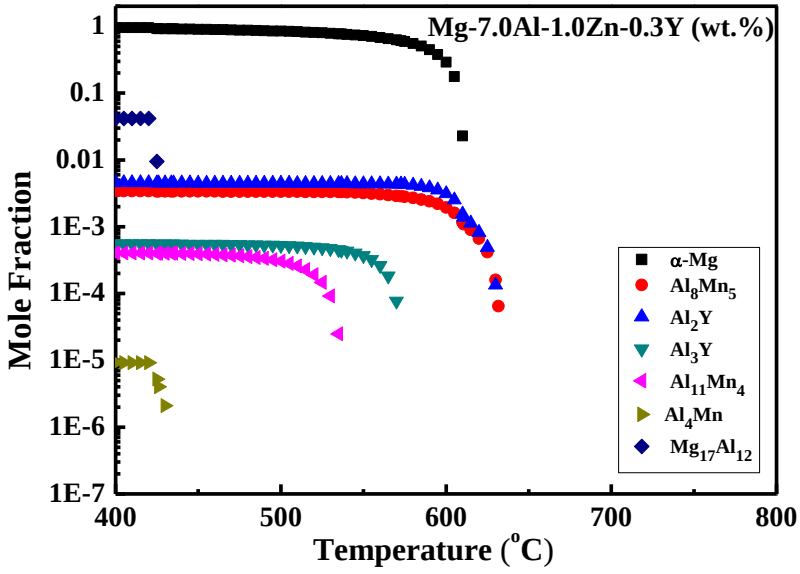

(d)

Figure 3.1(Continued) Solidification behaviors of high pressure die-cast alloys: (c) Mg-7.0Al-0.5Zn-0.3Y, (d) Mg-7.0Al-1.0Zn-0.3Y

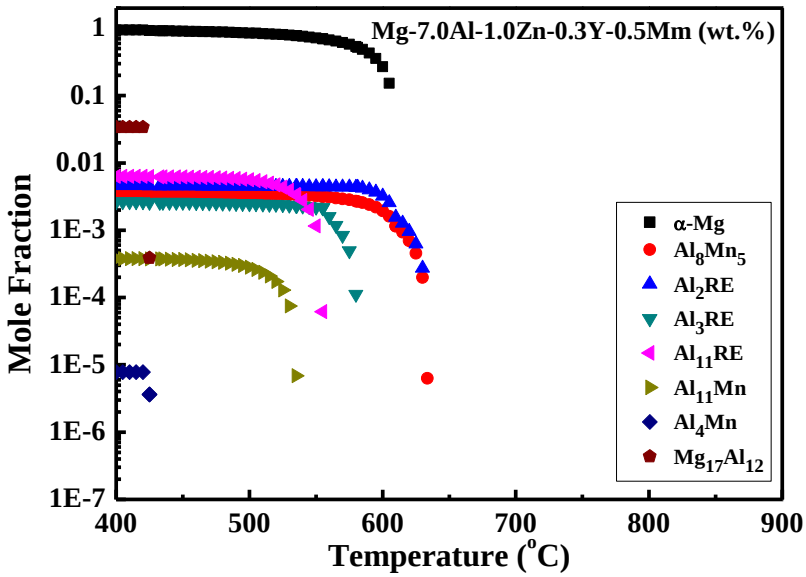

(e)

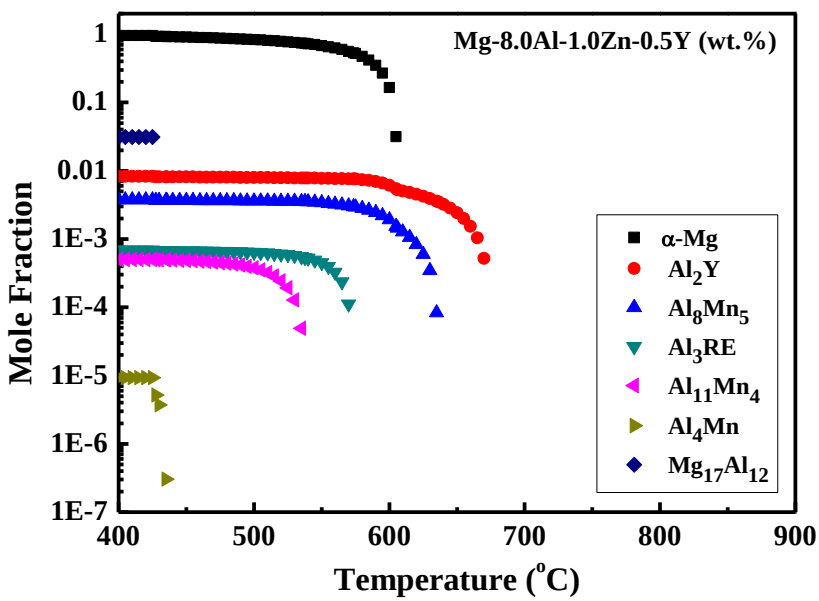

(f)

Figure 3.1(Continued) Solidification behaviors of high pressure die-cast alloys: (e) Mg-7.0Al-1.0Zn-0.3Y-0.5Mm, (f) Mg-8.0Al-1.0Zn-0.3Y

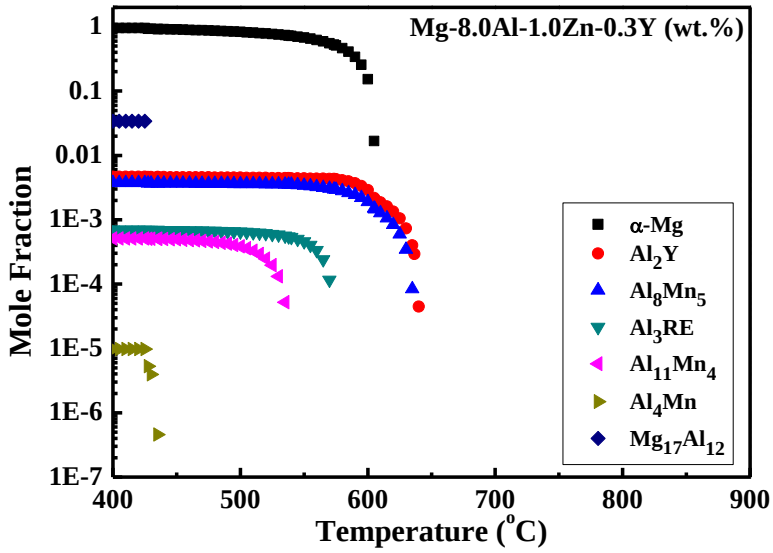

(g)

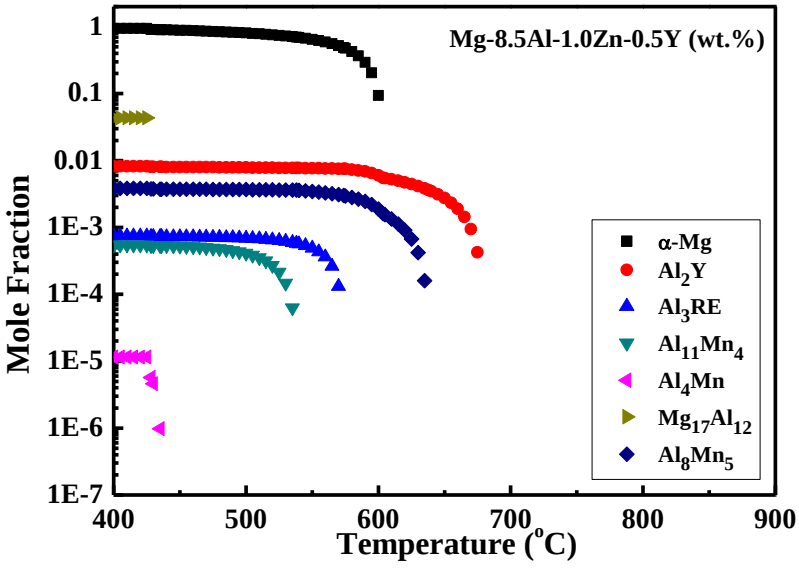

(h)

Figure 3.1(Continued) Solidification behaviors of high pressure die-cast alloys: (g) Mg-8.0Al-1.0Zn-0.5Y, (h) Mg-8.5Al-1.0Zn-0.5Y

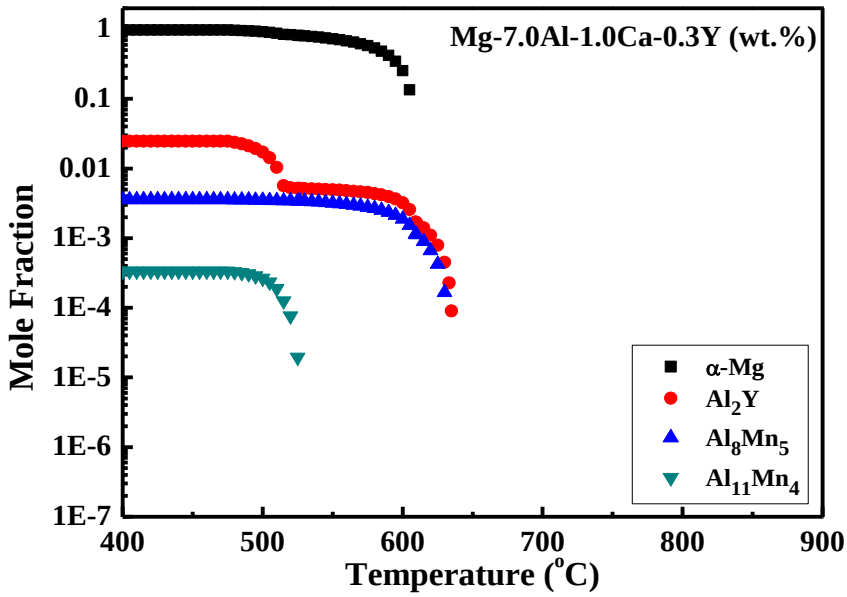

(i)

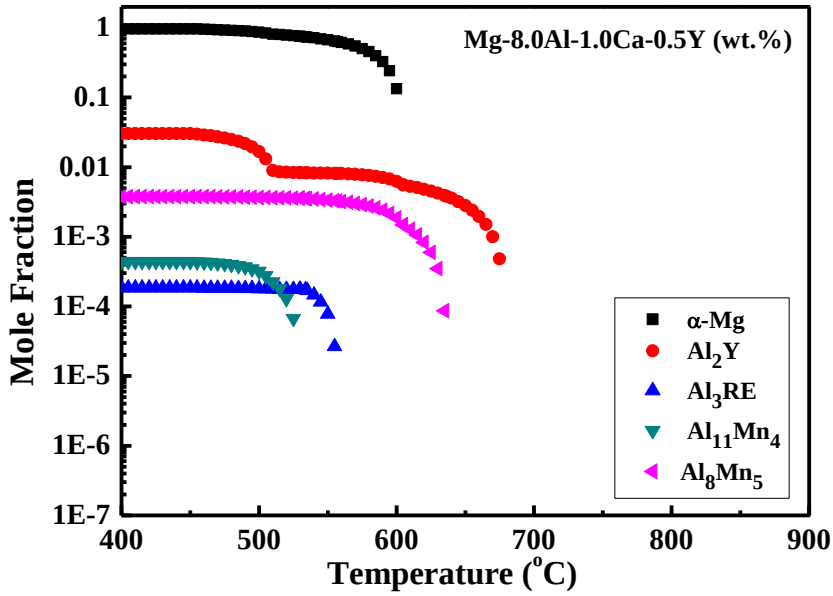

(j)

Figure 3.1(Continued) Solidification behaviors of high pressure die-cast alloys: (i) Mg-7.0Al-1.0Ca-0.3Y, (j) Mg-8.0Al-1.0Ca-0.5Y

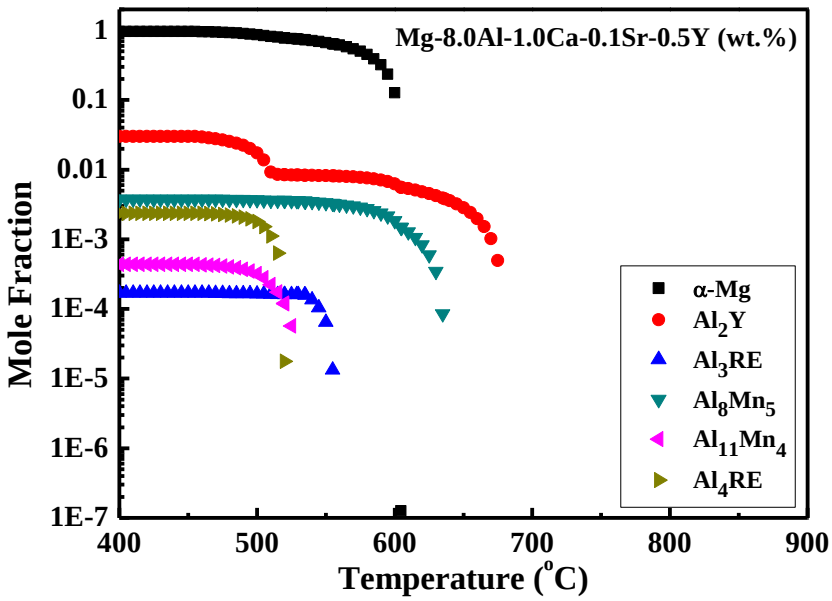

(k)

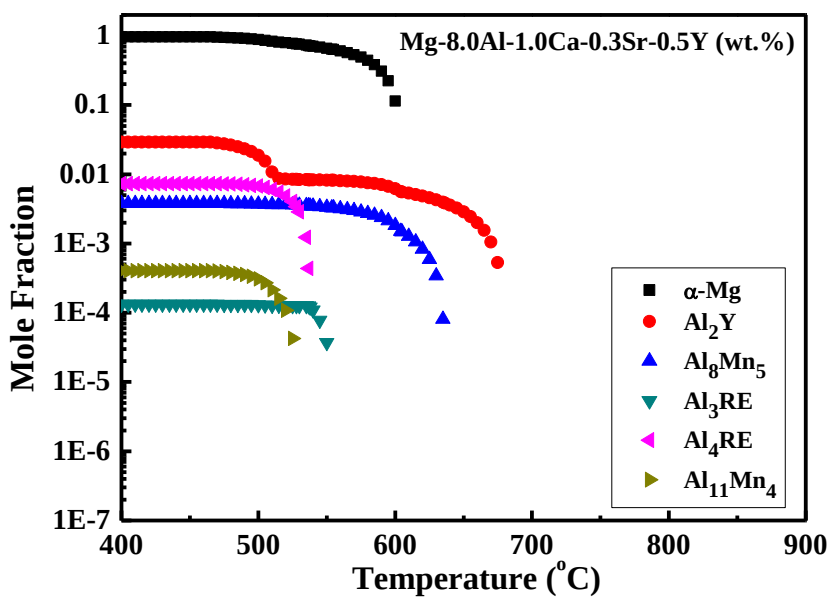

(l)

Figure 3.1(Continued) Solidification behaviors of high pressure die-cast alloys: (k) Mg-8.0Al-1.0Ca-0.1Sr-0.5Y, (l) Mg-8.0Al-1.0Ca-0.3Sr-0.5Y

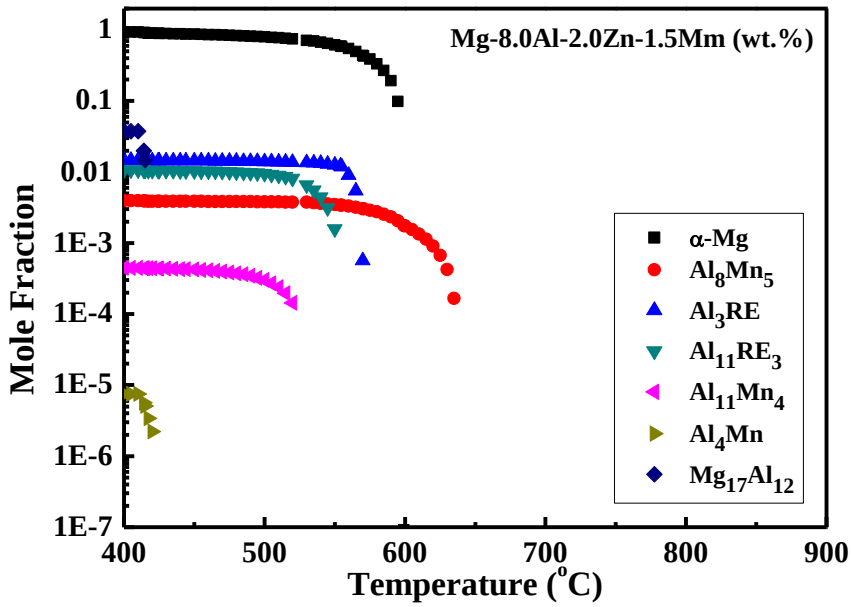

(m)

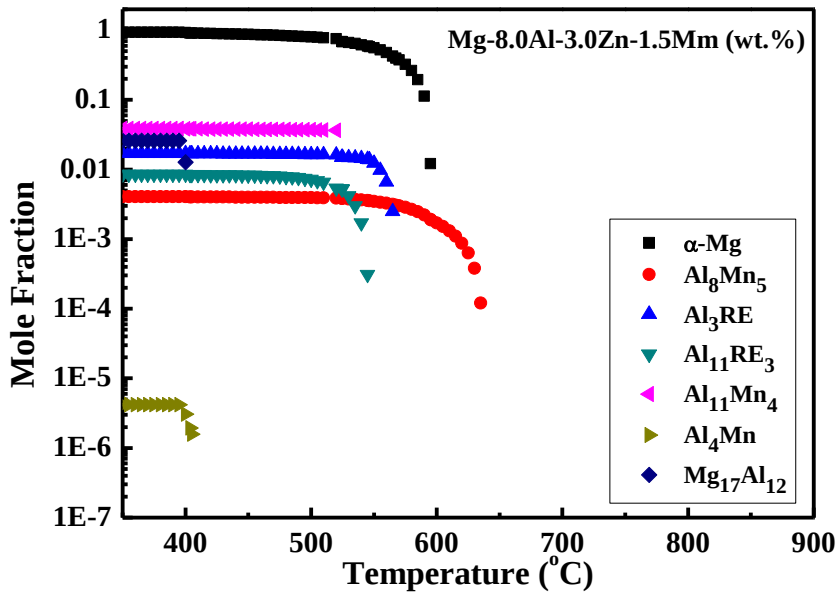

(n)

Figure 3.1(Continued) Solidification behaviors of high pressure die-cast alloys: (m) Mg-7.0Al-2.0Zn-0.5Mm, (n) Mg-7.0Al-3.0Zn-0.5Mm

Table 3.1 Mole fraction of each phase with different alloying elements in high pressure die-cast Mg-Al-Sn alloys

Alloy Systems	Amount of Phases at Room Temperature (wt.%)										
	$Mg_{17}Al_{12}$	Al_2RE	Al_3RE	Al_4Mn	$Al_{11}RE_3$	Al_8Mn_5	$Al_{11}Mn_4$	Al_4Sr	Ca_2Sn	Mg_2Sn	α-Mg
Mg-6.0Al-5.0Sn-0.6Ca-0.3Mn	-	-	-	-	-	0.86	0.03	-	2.29	0.42	Bal.
Mg-6.0Al-6.0Sn-0.75Ca-0.3Mn	-	-	-	-	-	0.87	0.03	-	3.00	0.92	Bal.
Mg-7.0Al-0.5Zn-0.3Y	2.09	0.47	0.05	7.63e-4		0.34	0.04	-	-	-	Bal.
Mg-7.0Al-1.0Zn-0.3Y	4.19	0.46	0.06	9.21e-4		0.34	0.04	-	-	-	Bal.
Mg-7.0Al-1.0Zn-0.3Y-0.5Mm	3.39	0.46	0.26	7.76e-4	0.63	0.35	0.04	-	-	-	Bal.
Mg-8.0Al-1.0Zn-0.3Y	3.39	0.47	0.07	9.76e-4	-	0.38	0.05	-	-	-	Bal.
Mg-8.0Al-1.0Zn-0.5Y	3.12	0.83	0.07	9.27e-4	-	0.38	0.05	-	-	-	Bal.
Mg-8.5Al-1.0Zn-0.5Y	4.35	0.82	0.07	1.15e-3	-	0.38	0.05	-	-	-	Bal.
Mg-7.0Al-1.0Ca-0.3Y	-	2.47	-	-	-	0.36	0.03	-	-	-	Bal.
Mg-8.0Al-1.0Ca-0.5Y	-	3.00	0.02	-	-	0.38	0.04	-	-	-	Bal.
Mg-8.0Al-1.0Ca-0.1Sr-0.5Y	-	3.00	0.02	-	-	0.38	0.04	0.24	-	-	Bal.
Mg-8.0Al-1.0Ca-0.3Sr-0.5Y	-	3.00	0.01	-	-	0.38	0.04	0.73	-	-	Bal.
Mg-7.0Al-2.0Zn-1.5Mm	3.76	1.47	-	7.52e-4	1.07	0.40	0.04	-	-	-	Bal.
Mg-7.0Al-3.0Zn-1.5Mm	2.60	-	1.71	4.18e-4	0.86	0.41	0.04	-	-	-	Bal.

3.2. Mechanical Properties at Room Temperature of As-casted Specimen

As referred before, the tensile test was carried out at room temperature. The yield strengths of die-cast Mg-Al based alloys were shown in Figure 3.2 and Table 3.2. The ultimate tensile strength of Mg-7.0Al-0.5Zn-0.3Y is 247.4MPa. By the addition of 1.0wt.% Zn to this composition, the ultimate tensile strength increase to 257.3MPa. After adding Mm to this alloy system, the elongation decreased to 5.5%. And change Zn element to Ca element, the elongation decreased as well.

In the case of AM60-5.0Sn-0.6Ca, this composition shows the highest elongation rate. In Mg-Sn-Ca system, the ratio of Sn/Ca decides the intermetallic

phases that form in the microstructure. When the ratio is higher than 2.5, Ca is almost totally bound to Mg and Sn to form MgCaSn phase, which is thermally stable and helps in increasing the creep strength of the alloy.

In those alloy system which include Y, with the increasing of the contents of Y, the elongation increased together. And Compared the properties of Mg-7.0Al-1.0Ca-0.3Y and Mg-8.0Al-1.0Ca-0.5Y, add more elements, the properties was improved.

The highest yield strength is 150.5MPa, which from Mg-8.5Al-1.0Zn-0.5Y, because of the existence of $Mg_{17}Al_{12}$ phase, the yield strength increased, but because of its brittleness, the elongation is very poor.

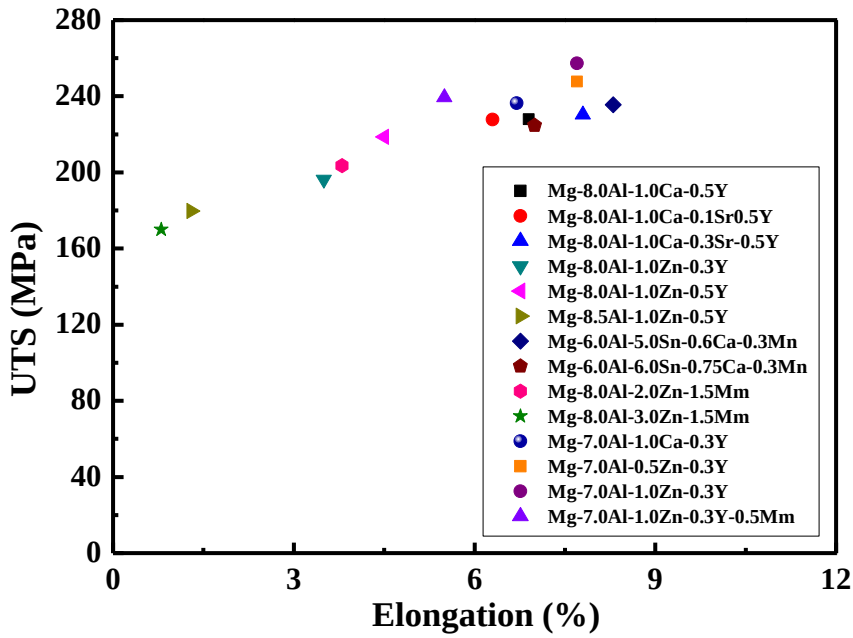

Figure 3.2 Ultimate Tensile Strength and Elongation of As-casted Specimen

Table 3.2 Mechanical properties of different compositions

Alloy Systems	Mechanical Properties (R.T.)		
	Yield Strength (MPa)	Ultimate Tensile Strength (MPa)	Elongation (%)
Mg-6.0Al-5.0Sn-0.6Ca-0.3Mn	145.5	235.6	8.3
Mg-6.0Al-6.0Sn-0.75Ca-0.3Mn	146.5	224.7	7.0
Mg-7.0Al-0.5Zn-0.3Y	146.4	237.4	7.7
Mg-7.0Al-1.0Zn-0.3Y	148.6	237.3	7.7
Mg-7.0Al-1.0Zn-0.3Y-0.5Mm	147.4	229.4	5.5
Mg-8.0Al-1.0Zn-0.3Y	139.8	196.2	3.5
Mg-8.0Al-1.0Zn-0.5Y	143.2	218.6	5.4
Mg-8.5Al-1.0Zn-0.5Y	150.5	179.7	1.3
Mg-7.0Al-1.0Ca-0.3Y	145.3	220.0	5.4
Mg-8.0Al-1.0Ca-0.5Y	144.7	239.3	7.7
Mg-8.0Al-1.0Ca-0.1Sr-0.5Y	148.3	237.7	6.3
Mg-8.0Al-1.0Ca-0.3Sr-0.5Y	145.3	230.3	7.8
Mg-8.0Al-2.0Zn-1.5Mm	147.1	203.1	3.1
Mg-8.0Al-3.0Zn-1.5Mm	143.8	169.9	0.8

3.3. Microstructure

The observation with an optical micrograph for high pressure die-cast MgAl-Sn based alloys is shown in Figure 3.3. As seen in Figure3.3 (a) and (b), after add more elements, the grain size was refined but the texture became not homogeneous, maybe this can explain why the properties get a little decreased.

After adding Mm to Mg-7.0Al-1.0Zn-0.3Y (Figure3.3 (c)(d)(e)) alloy system, the grain size got refinement obviously. Al_4RE (also reported as $AE_{11}RE_3$) lamellar phase dominates the interdendritic microstructure, which also contains minor amounts of particulate Al_2RE phase. The RE used in AE alloys consists primarily of cerium and lanthanum, which makes the Al_4RE in the alloys a mixture of Al_4Ce and Al_4La. Since these phases are present at the grain boundaries, they suppressed the growing of dendrite. On the other hand, adding more Zn is contribute to reduce dendrite arm spacing and the growing of grains.

As shown in Figure 3.3 (f) and (g), dendrite arm spacing was decreased with increasing Y contents. For comparison of Figure3.3 (j)(k)(l), for the refinement of grain, the optimal contents of Sr is 0.1wt.%.

Scanning electron microscopic studies were carried out in order to identify the second phase particles present in the alloy and are shown in Figure 3.4.

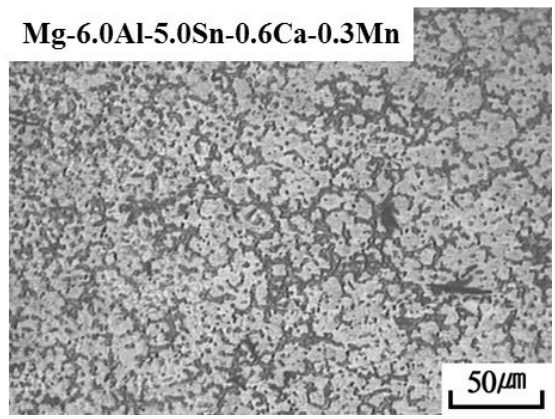

(a)

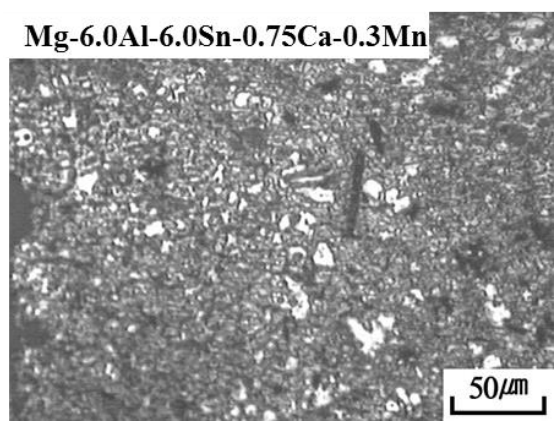

(b)

Figure 3.3 OM pictures of different compositions: (a) Mg-6.0Al-5.0Sn-0.6Ca-0.3Mn, (b) Mg-6.0Al-6.0Sn-0.75Ca-0.3Mn

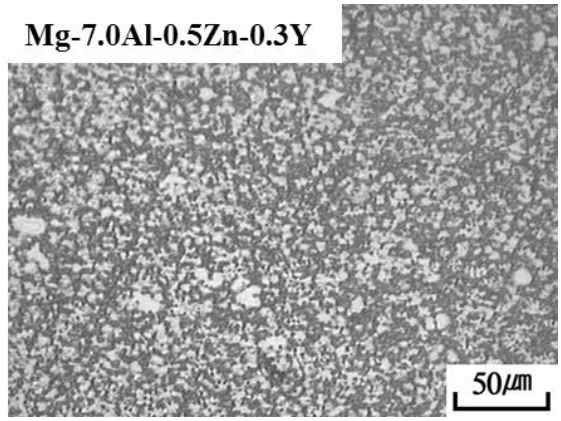

(c)

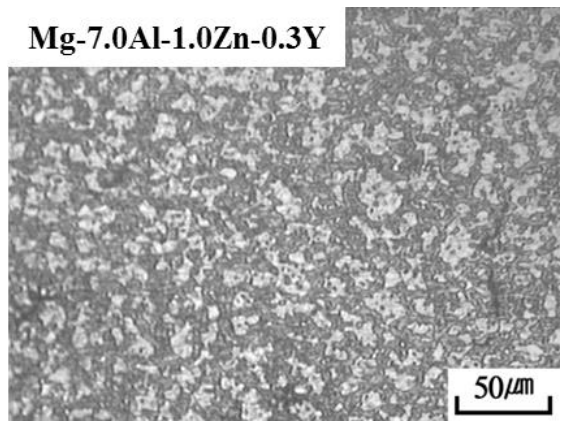

(d)

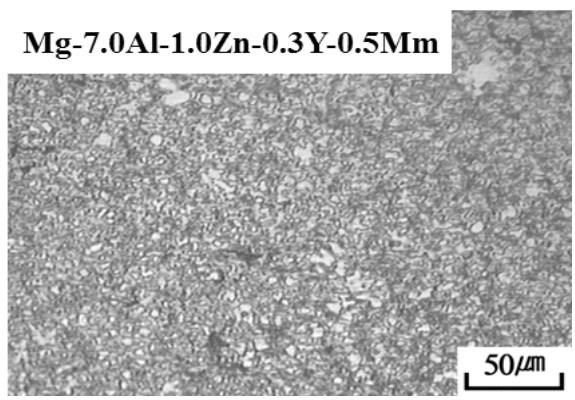

(e)

Figure 3.3(Continued) OM pictures of different compositions: (c) Mg-7.0Al-0.5Zn-0.3Y, (d) Mg-7.0Al-1.0Zn-0.3Y, (e) Mg-7.0Al-0.5Zn-0.3Y-0.5Mm

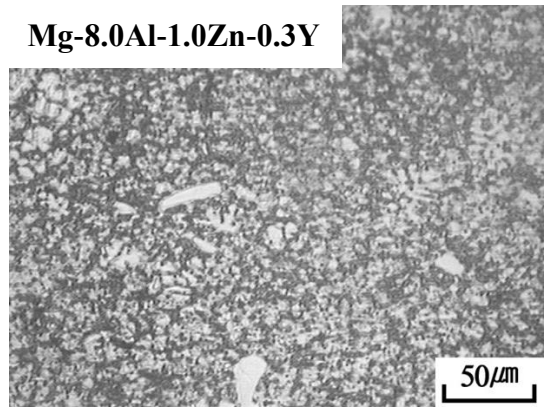

(f)

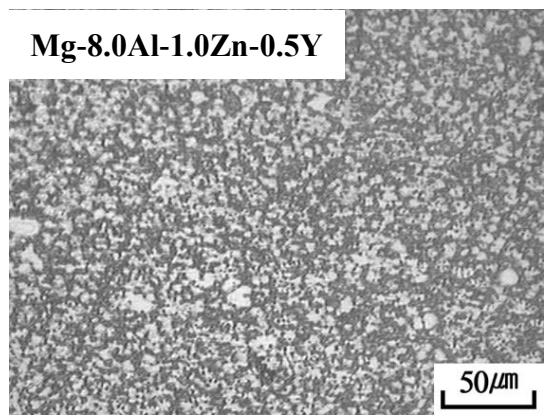

(g)

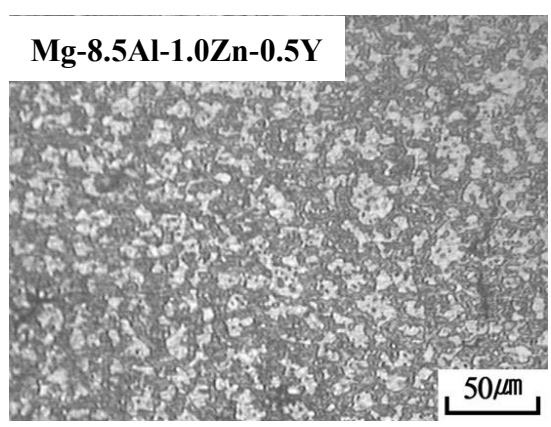

(h)

Figure 3.3(Continued) OM pictures of different compositions: (f) Mg-8.0Al-1.0Zn-0.3Y, (g) Mg-8.0Al-1.0Zn-0.3Y, (h) Mg-8.5Al-1.0Zn-0.5Y

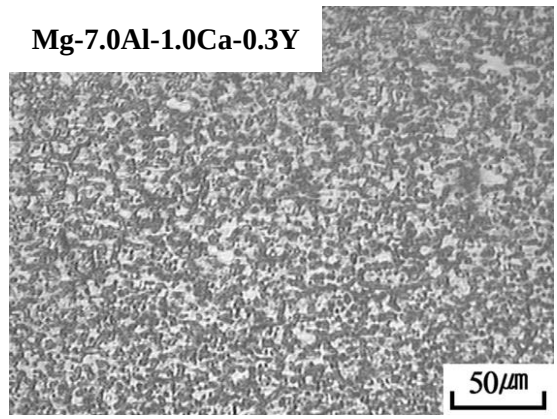

(i)

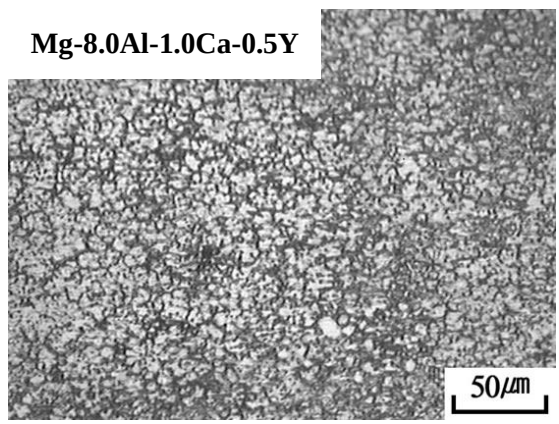

(j)

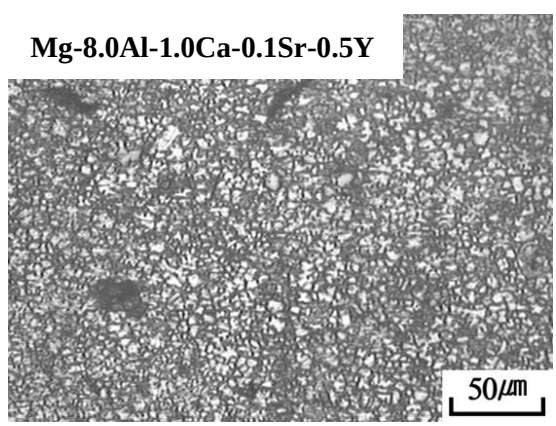

(k)

Figure 3.3(Continued) OM pictures of different compositions: (i) Mg-7.0Al-1.0Ca-0.3Y, (j) Mg-8.0Al-1.0Ca-0.5Y, (k) Mg-8.0Al-1.0Ca-0.1Sr-0.5Y

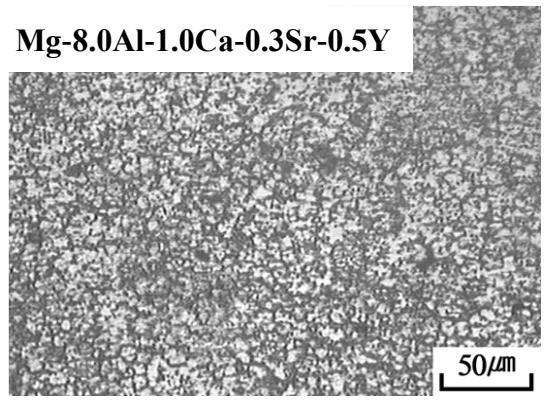

(l)

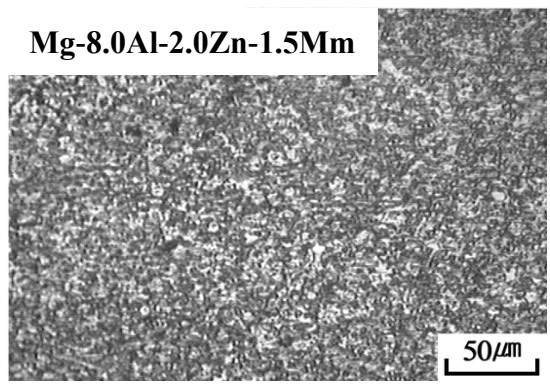

(m)

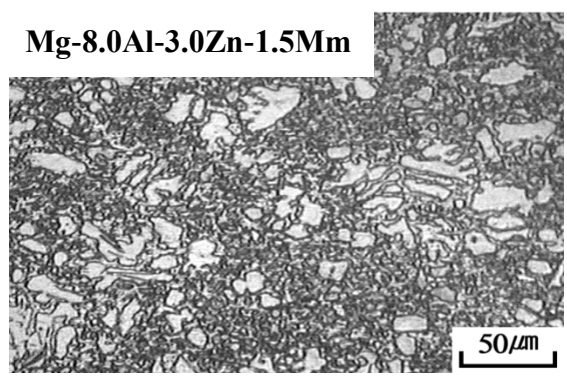

(n)

Figure 3.3(continued) OM pictures of different compositions: (l) Mg-8.0Al-1.0Ca-0.3Sr-0.5Y, (m) Mg-8.0Al-2.0Zn-1.5Mm, (n) Mg-8.0Al-3.0Zn-1.5Mm

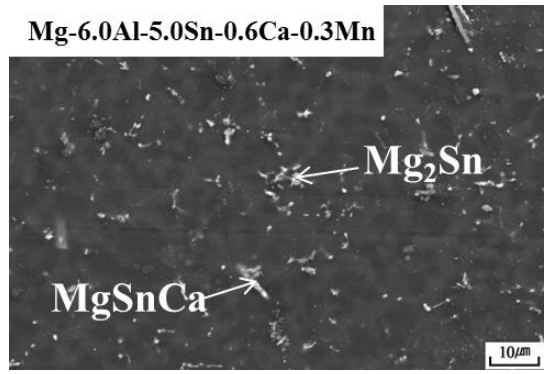

(a)

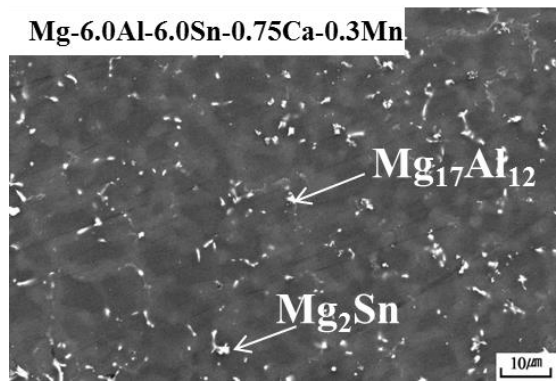

(b)

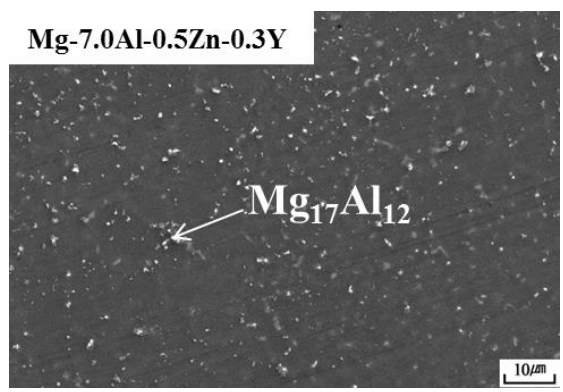

(c)

Figure 3.4 SEM and EDS analysis of different compositions: (a) AM60-5.0Sn-0.6Ca, (b) AM60-6.0Sn-0.75Ca, (c) Mg-7.0Al-0.5Zn-0.3Y

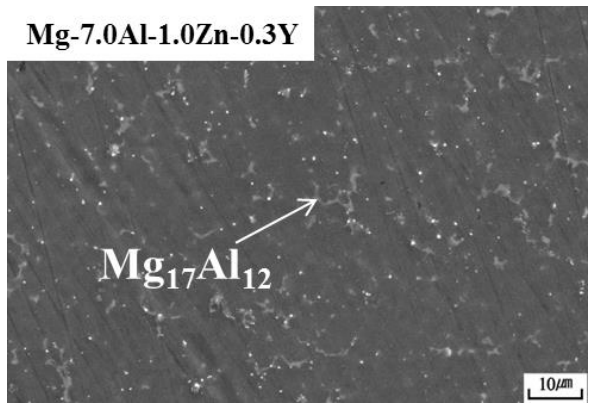

(d)

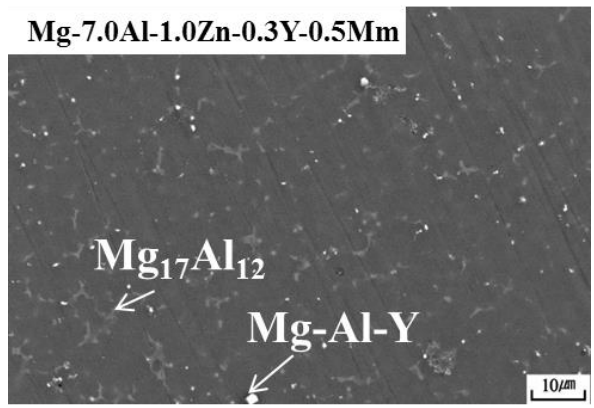

(e)

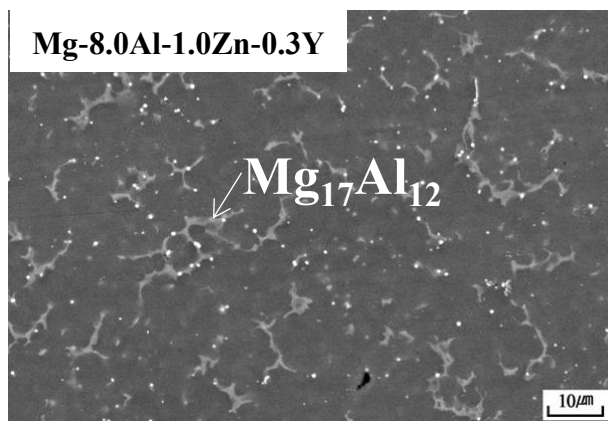

(f)

Figure 3.4(continued) SEM and EDS analysis of different compositions: (d) Mg-7.0Al-1.0Zn-0.3Y, (e) Mg-7.0Al-0.5Zn-0.3Y-0.5Mm, (f) Mg-8.0Al-1.0Zn-0.3Y

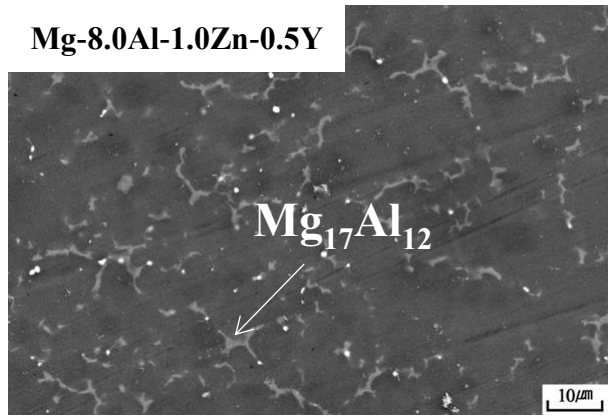

(g)

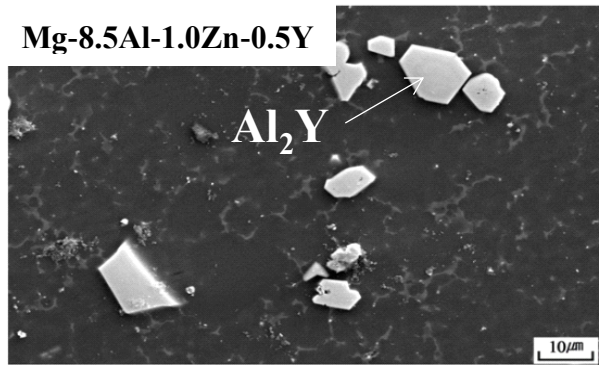

(h)

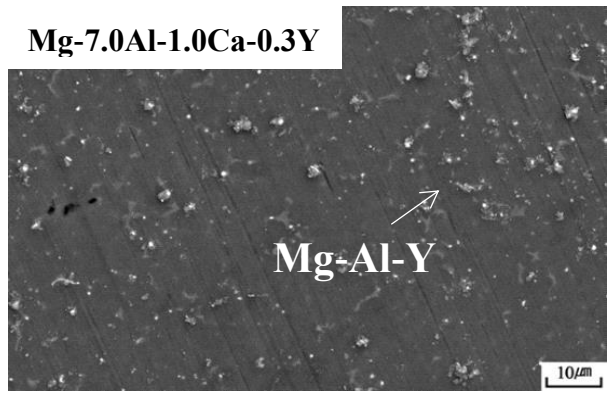

(i)

Figure 3.4(continued) (g) Mg-8.0Al-1.0Zn-0.3Y, (h) Mg-8.5Al-1.0Zn-0.5Y, (i) Mg-7.0Al-1.0Ca-0.3Y

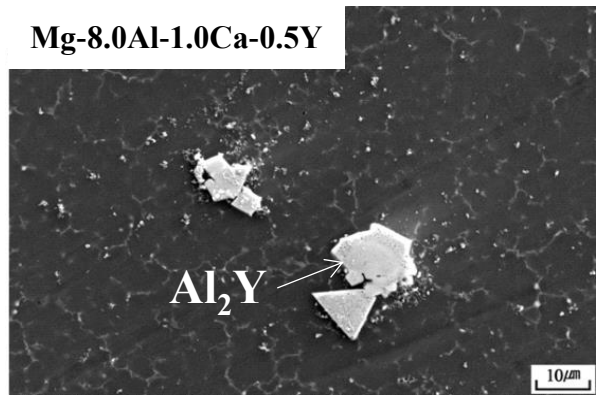

(j)

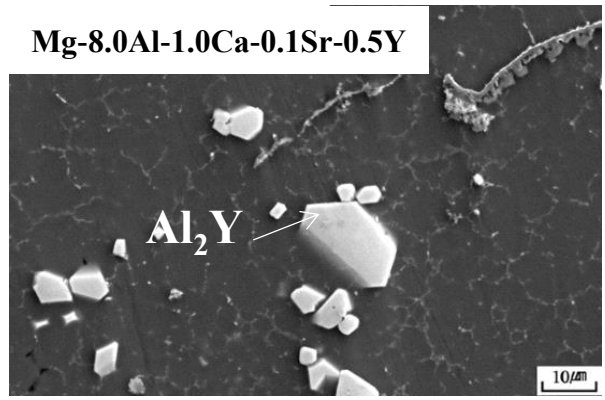

(k)

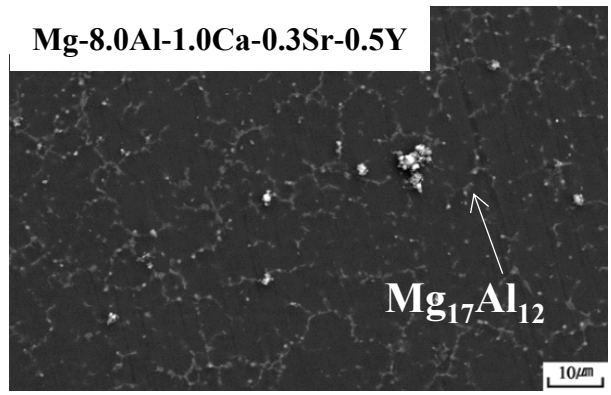

(l)

Figure 3.4(continued) OM pictures of different compositions: (j) Mg-8.0Al-1.0Ca-0.5Y, (k) Mg-8.0Al-1.0Ca-0.1Sr-0.5Y, (l) Mg-8.0Al-1.0Ca-0.3Sr-0.5Y

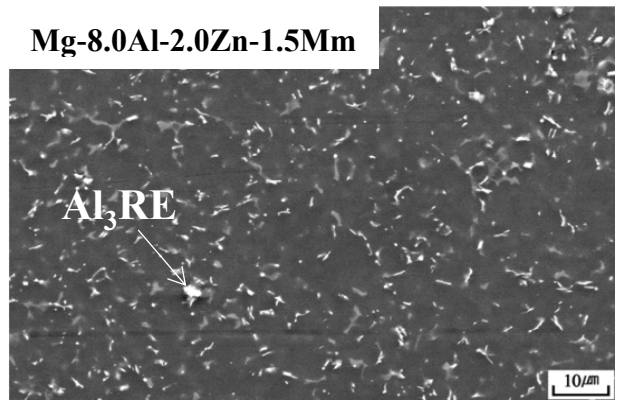

(m)

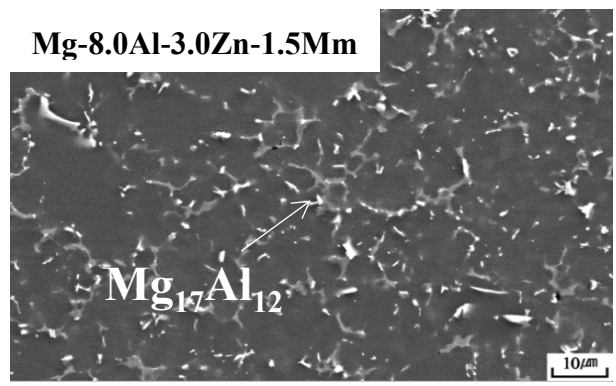

(n)

Figure 3.4(continued) OM pictures of different compositions: (m) Mg-8.0Al-2.0Zn-1.5Mm, (n) Mg-8.0Al-2.0Zn-1.5Mm

It was confirmed by the SEM analyses that the there was no second phases were $Mg_{17}Al_{12}$ in the AM60 system alloy. From the EDS analysis, it is evident that the matrix is a-Mg, and the white precipitate is the Mg_2Sn phase. And the MgCaSn phase was observed in the AM60-5.0Sn-0.6Ca alloy as well. Presence of the CaMgSn phase at dendrite interior and boundaries could act as a crack initiation site. Therefore, it can give a minor effect on the mechanical properties of die-cast alloys.

When the content of Al raised to 8wt. %, the $Mg_{17}Al_{12}$ can be observed obviouly. And those composition which include Ca, there was no $Mg_{17}Al_{12}$ phase can be observed. It evidenced that Ca has an effect on suppressed $Mg_{17}Al_{12}$ phase.

In Figure 3.4 (j)(k)(l), Al_2Y can be observed in (j) and (k), but (l). The same as simulated Al_4Sr was increased a lot, and the phase of Al_2Y decreased. Because of the existence of Al_2Y phase, the former composition has better properties than last one.

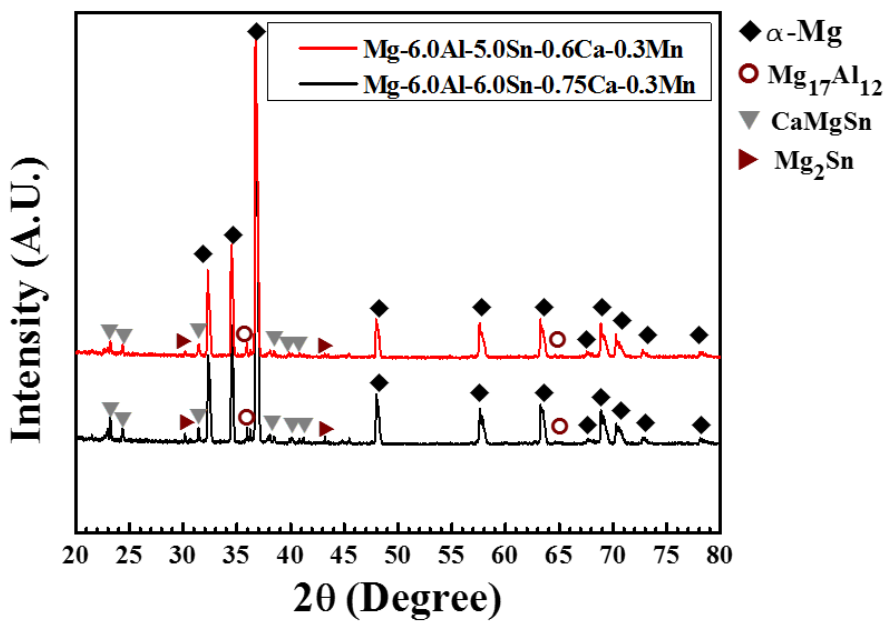

(a)

Figure 3.5 XRD analysis results of different alloy system: (a) Mg-6.0Al-XSn-XCa-0.3Mn alloy system

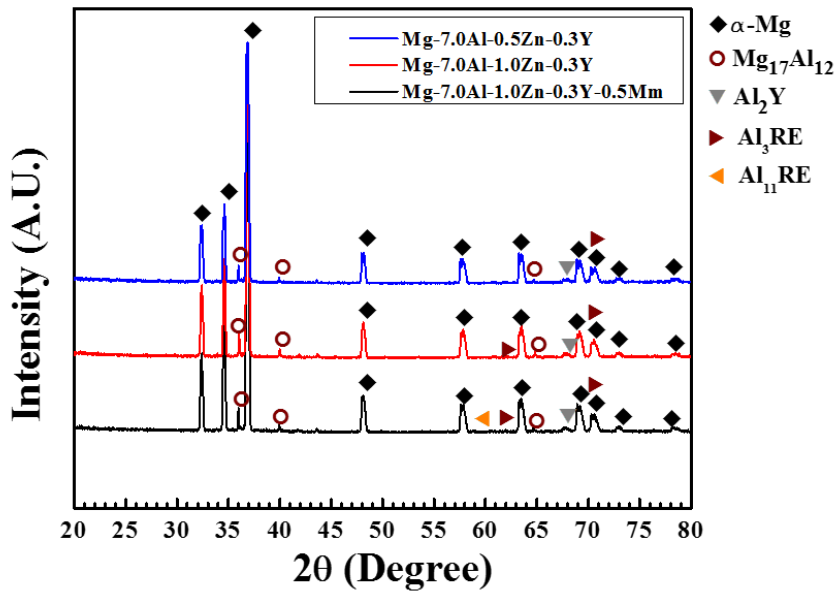

(b)

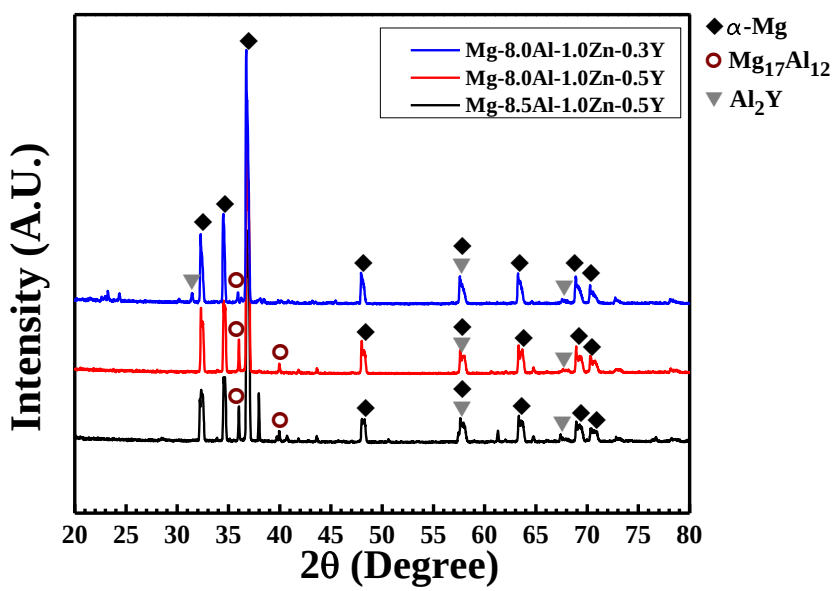

(c)

Figure 3.5(continued) XRD analysis results of different alloy system: (b) Mg-7.0Al-1.0Zn-XY alloy system, (c) Mg-8.0Al-1.0Zn-XY alloy system

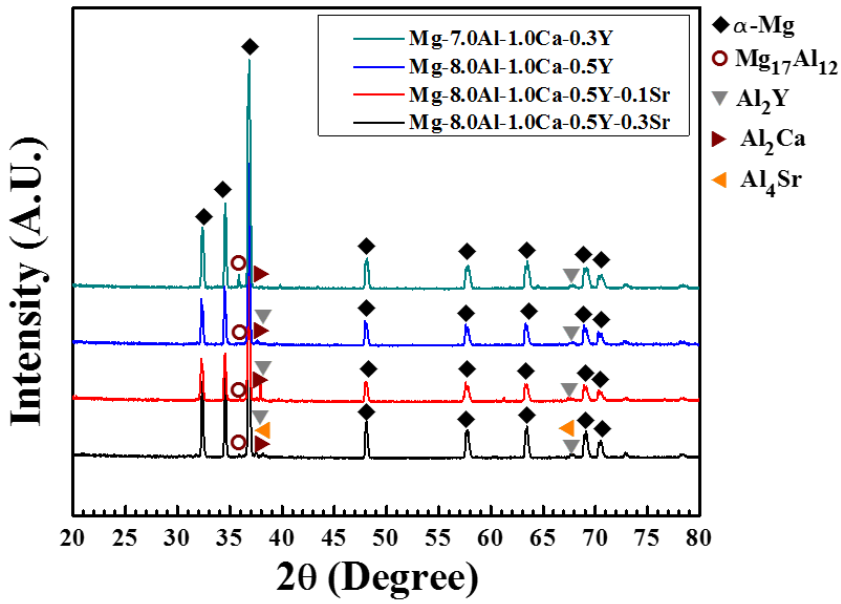

(d)

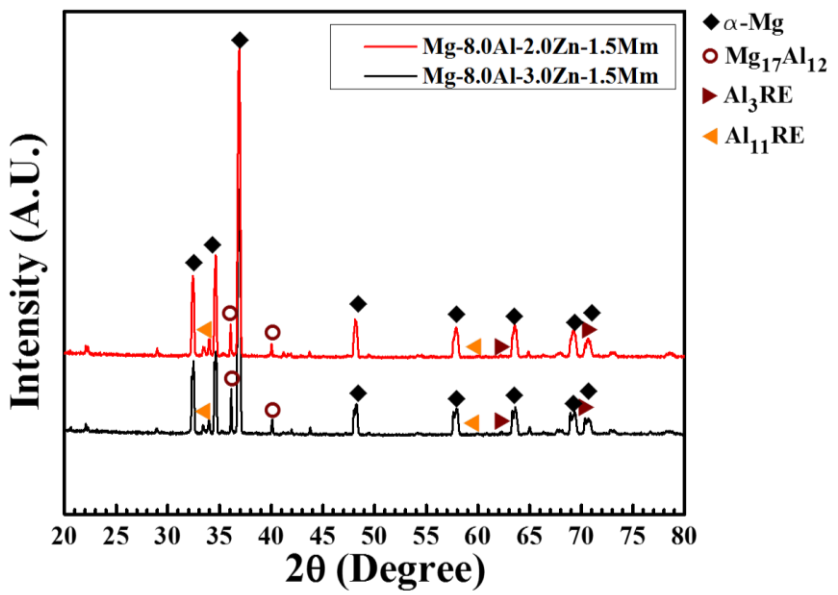

(e)

Figure 3.5(continued) XRD analysis results of different alloy system: (d) Mg-8.0Al-1.0Ca-XY alloy system, (e) Mg-8.0Al-XZn-1.5Mm alloy system

In this experiment, XRD was used for phase observation. Figure 3.5 shows the phase analysis results of different alloy. As observed in thermodynamic calculations and microstructures, the Mg_2Sn, CaMgSn phase was observed in Mg-6.0Al-Sn series alloys. And typical phase of Mg-Al alloys which include Y, Sr element Al_2Y, Al_4Sr were observed. These phase are benefit for improve strength by precipitate strengthening.

Even though the yield strength of die-cast Mg alloys has importance as a criterion compared to the tensile strength and elongation in near net shape die-cast applications, the tensile strength and elongation have importance due to tensile stability especially in high pressure die-cast Mg alloys. The tensile strength and elongation in cast materials is strongly dependent on casting defects, therefore, effects of casting defects including gas pores and shrinkage pores on tensile stability of die-cast Mg-Al-Sn based alloys should be discussed.

From the Figure 3.5, the composition with the best property, Mg-7.0Al-1.0Zn-0.3Y, has the most fraction of ductile fracture, and the same in Mg-8.0Al-1.0Ca-0.5Y. The fraction of dimple are corresponded to the elongation results.

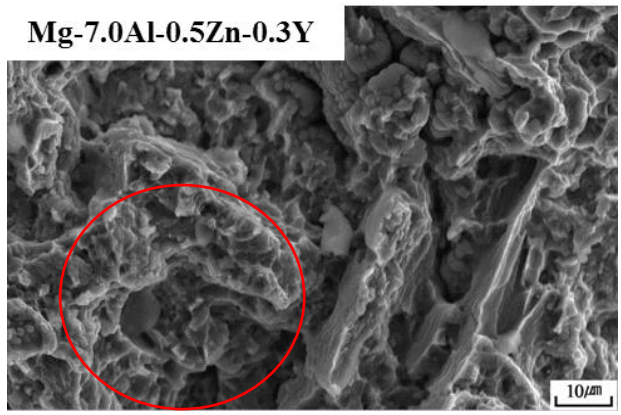

(a)

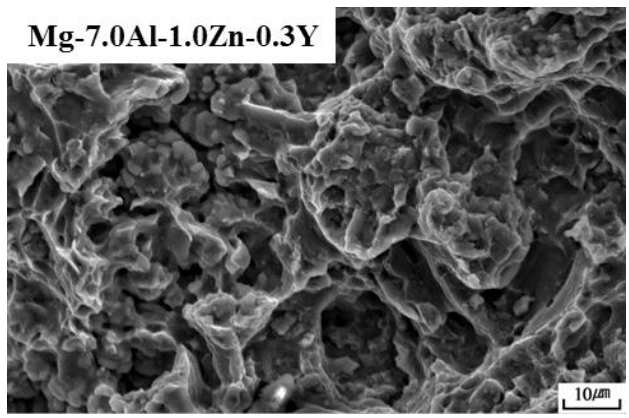

(b)

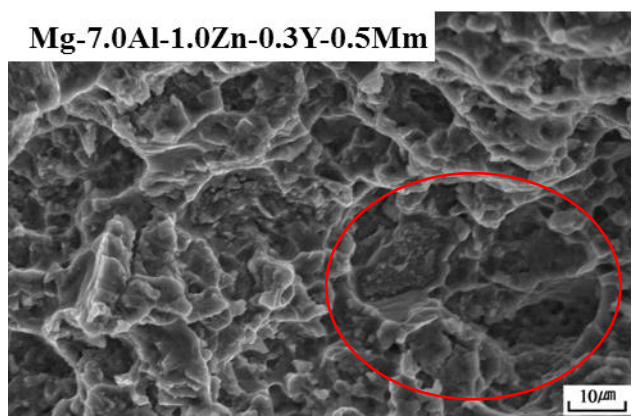

(c)

Figure 3.6 SEM pictures of section part after tensile test: (a) Mg-7.0Al-0.5Zn-0.3Y (b) Mg-7.0Al-1.0Zn-0.3Y (c) Mg-7.0Al-1.0Zn-0.3Y-0.5Mm

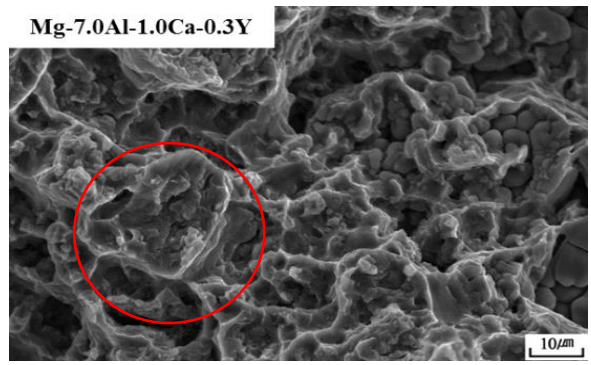

(d)

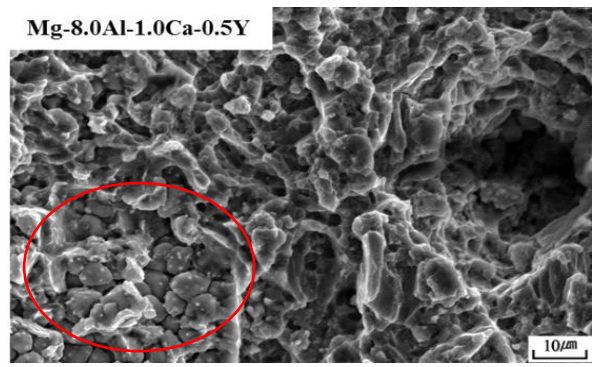

(e)

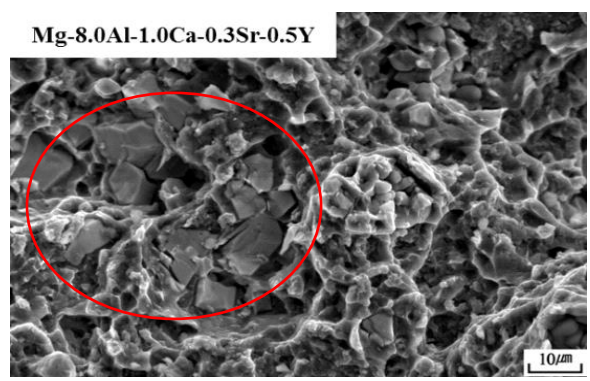

(f)

Figure 3.6(continued) (d) Mg-7.0Al-1.0Ca-0.3Y, (e) Mg-8.0Al-1.0Ca-0.3Y, (f) Mg-8.0Al-1.0Ca-0.3Sr-0.5Y

3.4. Mechanical Properties at Room Temperature after heat treatment

After heat treatment at120 ^{o}C in 0.5h, 1h, 2h, 4h, 8h, 12h, the tensile test was carried out at room temperature.

Notwithstanding no marked difference in the microstructure were detected, it was found that all the analyzed properties are significantly affected by the heat treatment. In particular, both UTS and YS do not change a lot in Mg-7.0Al-0.5Zn-X system alloys. Because of those phase which include Zn exhibits a brittle fracture, while the phase with more Al reveals a more ductile behavior after heat treatment.

In the case of Mg-6.0Al-5.0Sn-0.6Ca-0.3Mn, this composition shows the highest elongation rate. In Mg-Sn-Ca system, because of the Mg_2Sn, Mg_2Ca are thermal stable phase, and after heat treatment, those strength were much improved have very fine and homogenous microstructure (3.11(c) and (f)). After heat treatment, the YS and UTS were improved 15MPa.

In those alloy system which include Y and Ca, after heat treatment, the YS was improved 22.5MPa, the UTS was increased around 30MPa. In these cases, because of thermal stable strengthening phases Al_2Y and Al_4RE, the mechanical properties were increased significantly.

Table 3.3 Mechanical properties of different time after heat treatment

Alloy Systems& Heat Treatment	Mechanical Properties (R.T.)		
	Yield Strength (MPa)	Ultimate Tensile Strength (MPa)	Elongation (%)
Mg-6.0Al-5.0Sn-0.6Ca-0.3Mn, 0h at 120°C	145.5	237.7	8.9
Mg-6.0Al-5.0Sn-0.6Ca-0.3Mn, 0.5h at 120°C	161.3	250.4	6.9
Mg-6.0Al-5.0Sn-0.6Ca-0.3Mn, 1.0h at 120°C	156.2	187.1	1.8
Mg-6.0Al-5.0Sn-0.6Ca-0.3Mn, 2.0h at 120°C	160.2	238.2	6.0
Mg-6.0Al-5.0Sn-0.6Ca-0.3Mn, 4.0h at 120°C	156.1	245.9	7.0
Mg-6.0Al-5.0Sn-0.6Ca-0.3Mn, 8.0h at 120°C	161.3	245.6	6.7
Mg-6.0Al-5.0Sn-0.6Ca-0.3Mn, 12.0h at 120°C	160.1	230.9	5.2

Table 3.4 Mechanical properties of different time after heat treatment

Alloy Systems& Heat Treatment	Mechanical Properties (R.T.)		
	Yield Strength (MPa)	Ultimate Tensile Strength (MPa)	Elongation (%)
Mg-8.0Al-1.0Ca-0.5Y, 0h at 120°C	146.6	226.8	6.9
Mg-8.0Al-1.0Ca-0.5Y, 0.5h at 120°C	158.7	249.7	7.0
Mg-8.0Al-1.0Ca-0.5Y, 1.0h at 120°C	162.3	249.3	6.5
Mg-8.0Al-1.0Ca-0.5Y, 2.0h at 120°C	165.1	249.9	6.7
Mg-8.0Al-1.0Ca-0.5Y, 4.0h at 120°C	165.9	232.9	4.8
Mg-8.0Al-1.0Ca-0.5Y, 8.0h at 120°C	164.1	262.2	7.8
Mg-8.0Al-1.0Ca-0.5Y, 12.0h at 120°C	167.2	262.1	8.1

Table 3.5 Mechanical properties of different time after heat treatment

Alloy Systems& Heat Treatment	Mechanical Properties (R.T.)		
	Yield Strength (MPa)	Ultimate Tensile Strength (MPa)	Elongation (%)
Mg-8.0Al-1.0Ca-0.1Sr-0.5Y, 0h at 120°C	148.3	227.7	6.3
Mg-8.0Al-1.0Ca-0.1Sr-0.5Y, 0.5h at 120°C	161.4	251.6	7.2
Mg-8.0Al-1.0Ca-0.1Sr-0.5Y, 1.0h at 120°C	158.7	254.4	7.4
Mg-8.0Al-1.0Ca-0.1Sr-0.5Y, 2.0h at 120°C	162.3	254.0	7.1
Mg-8.0Al-1.0Ca-0.1Sr-0.5Y, 4.0h at 120°C	169.1	242.0	5.3
Mg-8.0Al-1.0Ca-0.1Sr-0.5Y, 8.0h at 120°C	202.2	239.7	3.1
Mg-8.0Al-1.0Ca-0.1Sr-0.5Y, 12.0h at 120°C	164.7	256.7	7.1

After heat treatment, from the microstructure observation, the grain size was refined and the whole microstructure got more homogenous. Those are the reasons of improvement of mechanical properties. At the beginning of heat treatment, the dendrite started to grow with the DAS decreased. After heat treatment 8h, the microstructure get homogenous and stable.

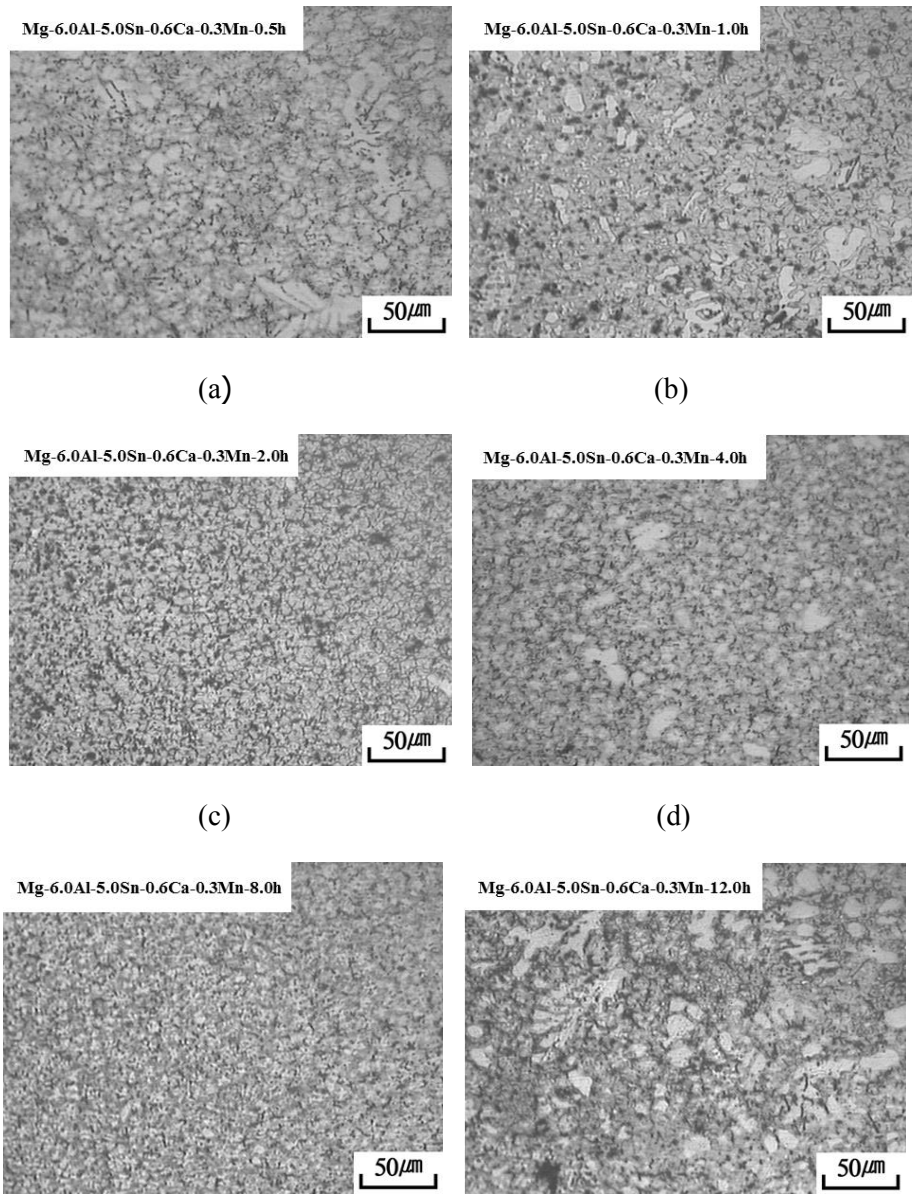

Figure 3.7 The microstructure of Mg-6.0Al-5.0Sn-0.6Ca-0.3Mn after heat treatment for (a) 0.5h, (b) 1h, (c) 2h, (d) 4h, (e) 8h, (f) 12h

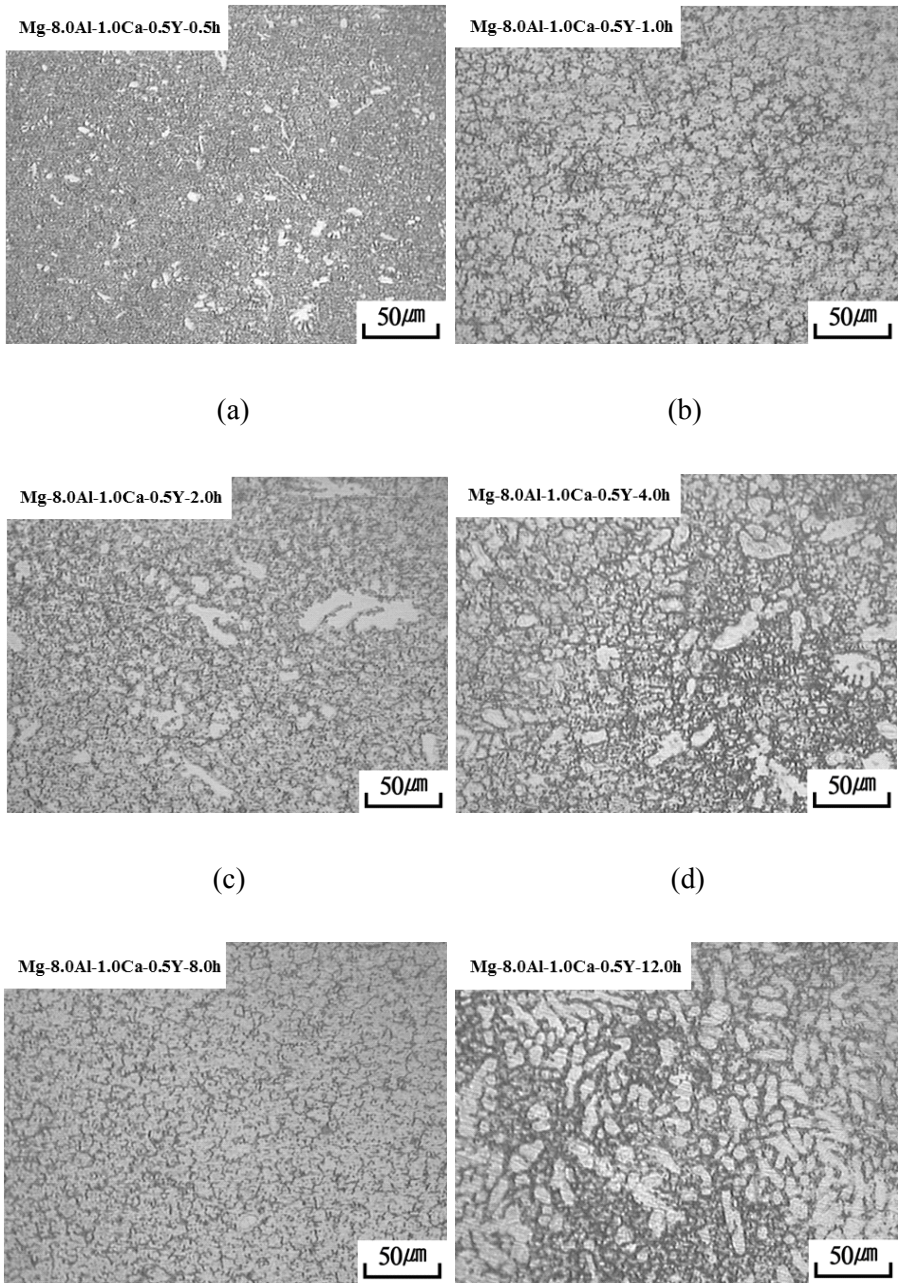

Figure 3.8 The microstructure of Mg-8.0Al-1.0Ca-0.5Y after heat treatment for (a) 0.5h, (b) 1h, (c) 2h, (d) 4h, (e) 8h, (f) 12h

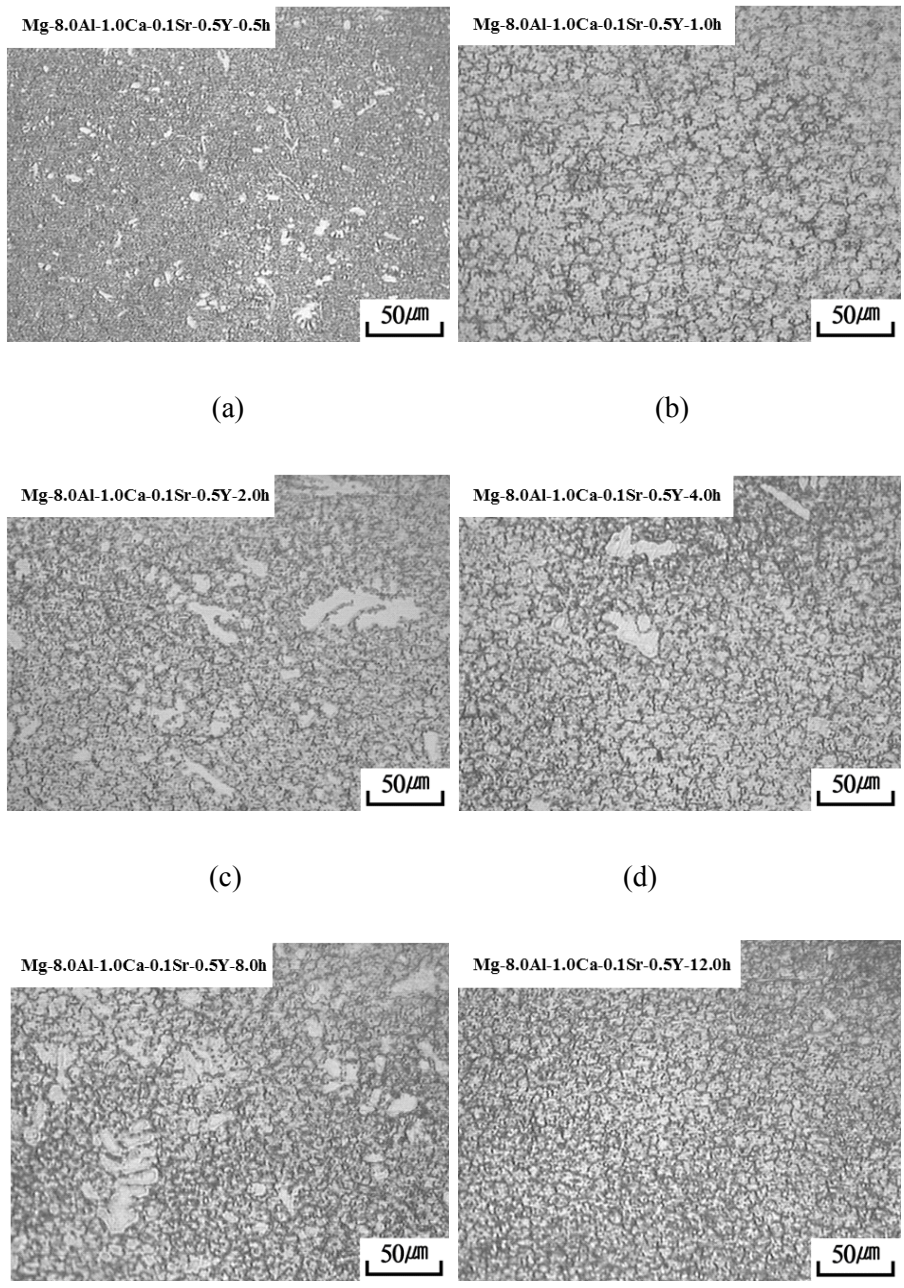

Figure 3.9 The microstructure of Mg-8.0Al-1.0Ca-0.5Y-0.1Sr after heat treatment for (a) 0.5h, (b) 1h, (c) 2h, (d) 4h, (e) 8h, (f) 12h

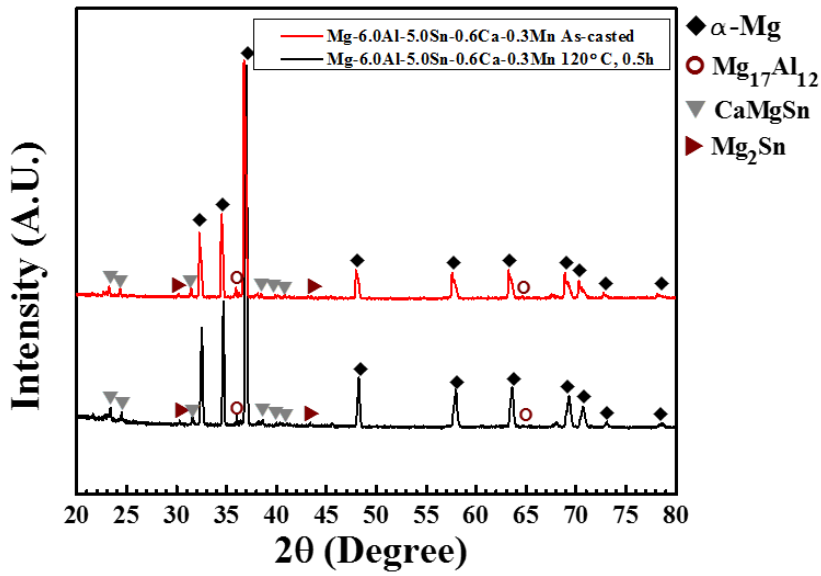

(a)

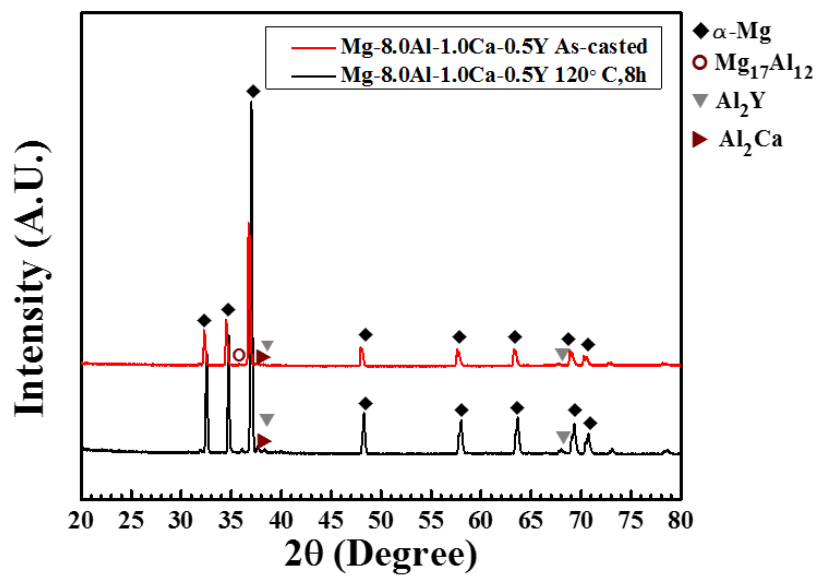

(b)

Figure 3.10 Comparison of XRD analysis results before and after heat treatment: (a) Mg-6.0Al-5.0Sn-0.6Ca-0.3Mn, (b) Mg-8.0Al-1.0Ca-0.5Y

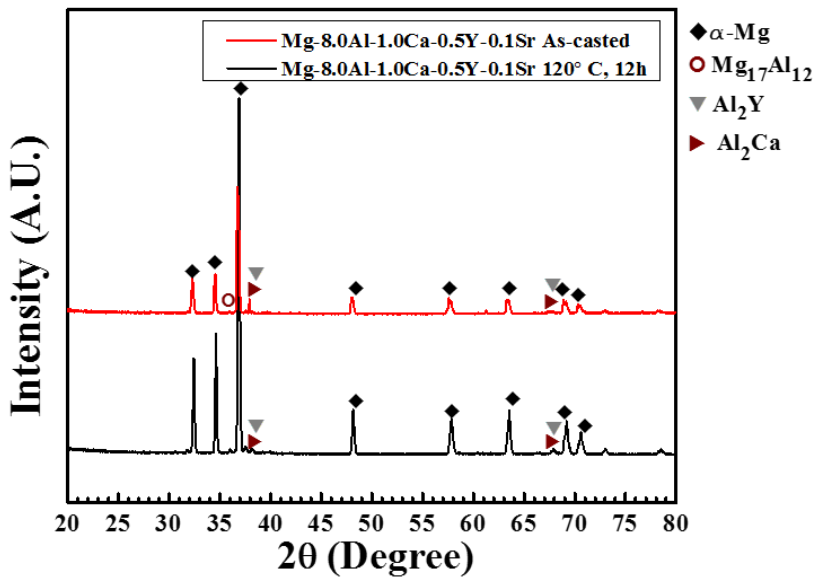

(c)

Figure 3.10(continued) Comparison of XRD analysis results before and after heat treatment: (c) Mg-8.0Al-1.0Ca-0.5Y-0.1Sr

XRD patterns of heat treated Mg-Al based alloys compared to as-cast alloys are shown in Figure 3.10. First of all, because the specimen were heat treated in low temperature 120 °C, the phase precipitated more. In the case of the Mg-6.0Al-5.0Sn-0.6Ca-0.3Mn alloy, the Mg_2Sn, CaMgSn and Al_2Ca phase is still remaining after heat treatment. In comparison of thermal stability of Mg_2Sn and CaMgSn phases, the CaMgSn phase is known to more stable rather than that of the Mg_2Sn phase []. The Al_2Ca phase is known as effective strengthener in the diecast Mg alloys which require heat resistance.

IV. Conclusions

In this study, mechanical properties of high pressure die-cast Mg-Al based alloys were investigated in the viewpoint of effects of microstructural changes by the addition of alloying elements. Conclusions are presented as follows:

1. From the thermodynamic calculations, the Al_8Mn_5 phase was initially precipitated first, and then the α-Mg was formed in the AM60 based alloy. By the addition of Ca to the AM60 alloy, CaMgSn and Mg_2Sn phases were precipitated.

2. In case of the Mg-7.0Al based alloy, the Al_2Y phase was initially precipitated first, and then the Al_8Mn_5 was formed. Additional precipitates including Al-Y and Al-Mm related phases were also precipitated by the addition of Y and Mm.

3. In case of the Mg-8.0Al based alloy, the Al_2Y phase was initially precipitated first, and the amount of $Mg_{17}Al_{12}$ decreased with the contents increasing of Y. The same with Mg-7.0Al based alloy, additional precipitates including Al-Y, Al-Sr and Al-Mm related phases were also precipitated by the addition of Y, Sr and Mm.

4. As expected in the thermodynamic calculations, the addition of Sn to the die-cast AM60 alloy induces the formation of the Mg_2Sn phase at dendrite boundaries. In case of those alloys added Y, the Al_2Y, Al-Sr and Al-Mm

phase was observed.

5. For the observation of microstructure, adding Mm is benefit for fine the grain size, and formed homogeneous microstructure. But because of low fluidity, the sample behaved very low elongation. So that lower tensile strength was observed. With adding more Zn, in the microstructure coarse grains were easily observed.

6. As to the mechanical properties, the Mg-8.5Al-1.0Zn-0.5Y has highest yield strength is 150.5 MPa, but it showed bad elongation, the reason of this result is large amount of brittle phase $Mg_{17}Al_{12}$ precipitated. The highest UTS is 239.3 MPa from Mg-8.0Al-1.0Ca-0.5Y alloy. The best elongation is 8.3% form AM60-5.0Sn-0.6Ca alloy.

7. After heat treatment in 120 ºC for different time, the strength of all alloys are increased, and the elongation didn't decrease significantly. The best result is Mg-8.0Al-1.0Ca-0.5Y alloy after heat treatment 8h and 12h. After heat treatment, all the mechanical properties improved.

8. Thermally stable precipitates at dendrite boundaries after heat treatment at 120ºC for 12h, $Mg_{17}Al_{12}$ were precipitated, and the microstructure improved more homogenous. Microstructural characteristics enhance mechanical properties at room and elevated temperature.

Reference

[1] F. S. Pan, M. B. Yang and X. H. Chen, “A Review on Casting Magnesium Alloys: Modification of Commercial Alloys and Development of New Alloys” *Journal of Materials Science & Technology*, Vol. 32 (2016) pp. 1211-1221.

[2] M. L. Su, J. H. Zhang, Y. Feng, Y. J. Bai, W. Wang, Z. W. Zhang and F. C. Jiang, “Al-Nd Intermetallic Phase Stability and Its Effects on Mechanical Properties and Corrosion Resistance of HPDC Mg-4Al-4Nd-0.2Mn Alloy” *Journal of Alloys and Compounds*, Vol. 691 (2017) pp. 634-643.

[3] J. H. Zhang, S. J. Liu, Z. Leng, M. L. Zhang, J. Meng and R. Z. Wu, “Microstructures and Mechanical Properties of Heat-resistant HPDC Mg–4Al-based Alloys Containing Cheap Misch Metal” *Materials Science and Engineering A*, Vol. 528 (2011) pp. 2670-2677.

[4] J. H. Zhang, D. P. Zhang, Z. Tian, J. Wang and K. Liu, “Microstructures, Tensile Properties and Corrosion Behavior of Die-cast Mg–4Al-based Alloys Containing La and/or Ce” *Materials Science and Engineering A*, Vol. 489 (2008) pp. 113-119.

[5] X. Li, S. M. Xiong and Z. Guo, “On the Tensile Failure Induced by Defect Band in High Pressure Die Casting of AM60B Magnesium Alloy” *Materials Science & Engineering A*, Vol. 674 (2016) pp. 687-695.

[6] Q. Yang, K. Guan, B. S. Li, S. H. Lv, F. Z. Meng, W. Sun, Y. Q. Zhang, X. J. Liu and J. Meng, “Microstructural Characterizations on Mn-containing Intermetallic Phases in a High-pressure Die-casting Mg–4Al–4RE–0.3Mn Alloy”

Materials Characterization, Vol. 132 (2017) pp. 381-387.

[7] S. M. Liang, H. W. Zhang, M. X. Xia, R. S. Chen and E. H. Han, "Microstructure and Mechanical Properties of Melt-conditioned High-pressure Die-cast Mg-Al-Ca Alloy" *Transactions of Nonferrous Metals Society of China*, Vol. 20 (2010) pp. 1205-1211.

[8] ASTM B557M-06, Standard Test Method for Tension Testing Wrought and Cast Aluminum and Magnesium Alloy Products [Metric], ASTM International, (2006).

[9] Y. M. Kim, "Mg-Al-Sn계 다이캐스팅 마그네슘합금의 미세조직 및 기계적 특성 변화에 미치는 Ca의 영향" *Busan University*, (2010)

[10] H. J. Park, "A Study on Effect of Alloying Elements on the Mechanical Properties of Die-casting Mg-Al-X Alloys" *Seoul National University,* (2017)

[11] T. I. So, "A Study on Microstructure and Mechanical Properties of High Pressure Die-cast Magnesium Alloys" *Seoul National University*, (2015)

[12] X. Li, S. M. Xiong, Z. Guo, "Failure Behavior of High Pressure Die Casting AZ91D Magnesium Alloy" *Materials Science & Engineering A*, Vol. 672 (2016) pp. 216-225.

[13] J. Song, S. M. Xiong, M. Li, J. Allison, "The Correlation between Microstructure and Mechanical Properties of High-pressure Die-cast AM50 Alloy" Journal of Alloys and Compounds, Vol. 477 (2009) pp. 863-869.

[14] J. H. Zhang, S. J. Liu, Z. Leng, X. H. Liu, Z. Y. Niu, M. L. Zhang, R. Z. Wu, "Structure Stability and Mechanical Properties of High-pressure Die-cast Mg–Al–La–Y-based Alloy" *Materials Science & Engineering A*, Vol. 531 (2012) pp. 70-75.

[15] L. F. Hu, S. P. Chen, Y. Miao, Q. S. Meng, “Die-casting effect on surface characteristics of thin-walled AZ91D magnesium components” *Applied Surface Science*, Vol. 261 (2012) pp. 851-856.

[16] N. Hort, Y. Huang, T. A. Leil, P. Maier and K. U. Kainer, “Microstructural Investigations of the Mg-Sn-xCa System” *Advanced Engineering Materials*, Vol. 8 (2006) pp. 359-364.

[17] R. Arrabal, B. Mingo, A. Pardo, E. Matykina, M. Mohedano, M.C. Merino, A. Rivas c, A. Maroto, “Role of Alloyed Nd in the Microstructure and Atmospheric Corrosion of As-cast Magnesium Alloy AZ91” *Corrosion Science*, Vol. 97 (2015) pp. 38-48.

[18] F. Mert, C. Blawert, K. U. Kainer, N. Hort, “Influence of Cerium Additions on the Corrosion Behavior of High Pressure Die Cast AM50 alloy” *Corrosion Science*, Vol. 65 (2012) pp. 145-151.

[19] A. A. Luo, “Magnesium Casting Technology for Structural Applications” *Journal of Magnesium and Alloys*, Vol. 1 (2013) pp. 2-22.

[20] B. H. Kim, S. W. Lee, Y. H. Park and I. M. Park, “The Microstructure, Tensile Properties, and Creep Behavior of AZ91, AS52 and TAS652 Alloy” *Journal of Alloys and Compounds*, Vol. 493 (2010) pp. 502-506.

[21] M. S. Dargusch, G. L. Dunlop and K. Pettersen, “The Microstructure and Creep Behavior of Die Cast Magnesium AZ91 and AS21 Alloy” *Transaction of 19th International Die Casting Congress* (1997) pp. 131-137.

[22] J. F. Knott, “Micromechanisms of Fracture and the Fracture Toughness of Engineering Alloys” *Fracture*, Vol. 1 (1977) pp. 61-91.

[23] A. H. Cottrell, “Theory of Brittle Fracture in Steel and Similar Metals” *Transactions of the ASME*, Vol. 212 (1958) pp.192-203.

[24] M. Socjusz-Podosek, “Effect of yttrium on structure and mechanical properties of Mg alloys” *Materials Chemistry and Physics*, Vol. 80 (2003) pp. 472-475.

[25] K. Ozturk, Y. Zhong, A. A. Luo and Z. K. Liu, “Creep Resistant Mg-Al-Ca Alloys: Computational Thermodynamics and Experimental Investigation”, *JOM January* (2003), pp. 40-44

[26] X. P. Niu, B. H. Hu, I. Pinwill and H. Li, “Vacuum Assisted High Pressure Die Casting of Aluminum Alloys” *Journal of Materials Processing Technology*, Vol. 105 (2000) pp. 119-127..

[27] M. K. Kulekei, “Mg and Its Alloys Applications in Automotive Industry” *Advanced Manufacturing Technology*, Vol. 39 (2007) pp. 851-861.

[28] Y. J. Jung and K. S. Shin, “Effects of Precipitates and Alloying Element on Microstructure and High Temperature Properties of Mg-Al Alloys” *Materials Science Forum*, Vol. 475-479 (2005) pp. 537-540.

[29] C. D. Lee, “Defect Susceptibility of Tensile Strength to Microporosity Variation in As-Cast Magnesium Alloys with Different Grain Sizes” *Metals and Materials International*, Vol. 16 (2010) pp. 543-551.

초록

마그네슘합금은 높은 열전도도, 비강도 및 기계 가공성 등 우수한 특성을 가지고 있으며 일반적으로 고압 다이캐스팅(HPDC) 공정을 통해 제조되고 있다. 현재 스티어링휠, 엔진블록, 오일팬 등의 자동차 부품들은 다른 부품에 비해 기술적 어려움과 원가의 문제점을 가지고 있음에도 불구하고, 전체 자동차 무게에 있어 큰 비중을 차지하여 경량화 효과를 크게 얻을 수 있다. 본 연구에서는350 ton 진공 다이캐스팅 장비를 이용하여 Mg-Al 합금에 Sn, Ca, Sr, Y 및 Mm 의 원소들을 첨가하여 다양한 합금계를 제조하였으며 첨가 원소에 따른 다이캐스팅 시편의 미세조직 변화와 기계적 특성을 평가하였다.

또한 120°C에서 0.5, 1,2,4,8,12시간동안 열처리하고 기계특성 및 미세조직에 대해 고찰 했다. 본 연구에서 SEM 및 XRD등 분석 기계를 통해서 모두 시편들의 미세조직 하고 석출물을 분석하였다.

주요어: 고압 다이캐스팅, Mg-Al합금, 기계적 특성, 열처리